DEVELOPMENT OF TIME-DEPENDENT DENSITY FUNCTIONAL THEORY IN CHEMICAL AND SOLID-STATE PHYSICS

BY FAN ZHANG

A dissertation submitted to the
Graduate School—New Brunswick
Rutgers, The State University of New Jersey
in partial fulfillment of the requirements
for the degree of
Doctor of Philosophy
Graduate Program in Physics

Written under the direction of
Professor Kieron Burke
and approved by

_____

_____

_____

_____

_____

New Brunswick, New Jersey

October, 2005

ABSTRACT OF THE DISSERTATION

Development of time-dependent density functional theory in chemical and solid-state physics

by Fan Zhang

Dissertation Director: Professor Kieron Burke

Today, Density Functional Theory (DFT) is one of the most widely applied electronic structure methods. Time Dependent DFT (TDDFT), which is an extension of DFT, can calculate the excitation properties of the systems. It has been used in physics, chemistry and biology researches. Known for its rigor, reliability, and efficiency, TDDFT is the method of choice both now and for the future. This thesis explores the implements of TDDFT in chemical and solid-state physics, we show how to use TDDFT to solve the double excitation and scattering problems.

Acknowledgements

I thank my advisor, Professor Kieron Burke for his guidance and support over the years. Thanks also to members of our group, past and present, who have contributed considerably to my learning through numerous useful discussions during the course of my graduate study: Maxime Dion, Rene Gaudoin, Paul Hessler, Max Koentopp, Aiyan Lu, Neepa Maitra, Rudolph Magyar, Vazgen Shekoyan, Eunji Sim, Eugene Tsiper, Meta van Faassen, Mike Vitarelli, Adam Wasserman, Takeyce Whittingham, and Federico Zahariev.

Special thanks to Professor Robert Cave, for the helpful discussion on double excitations during the year he visiting our group.

Last, I thank my parents and my wife for their love and support.

Table of Contents

List of Tables

List of Figures

List of Abbreviations

BO	Born-Oppenheimer
C	correlation
CI	configuration interaction
DF	density functional
DFT	density functional theory
EXX	exact exchange
GGA	generalized gradient approximation
GSL	GNU scientific library
HF	Hartree-Fock
KS	Kohn-Sham
LDA	local density approximation
MO	molecular orbital
PBE	Perdew-Burke-Ernzerhof GGA functional
SC	self-consistent
SE	Schrödinger equation
SPA	single pole approximation
TDDFT	time-dependent density functional theory
X	exchange
XC	exchange-correlation
ΔSCF	Δ self-consistent field

Chapter 1
Electronic Structure Methods

Electronic structure calculations are now widely used and very successful in solving problems in many fields [1], such as geometry optimizations, calculation of excitation energies, and reactions on surfaces. Computational studies can help people understand the experimental results, testing theories and making predictions. When the systems are too expensive or technique-hard to study experimentally, the computational method can provide some useful help. Traditionally, electronic structure computation is based on the Schrödinger equation (SE); people use some numerical methods solving it and obtain the information of the system from the wavefunctions. But when system size becomes large, the computing cost increases exponentially as the number of electrons increases. So the exact wavefunction method is impossible to use for large system, and we must find some reliable computational method which is effective for the large size systems.

A promising and proved method widely used in computational physics and quantum chemistry since the 1990s is density functional theory (DFT) [2, 3]. DFT produces good energetic while scaling favorably with electron number. With the advent of DFT and its implementation in electronic structure calculations on even larger systems are feasible. In addition, DFT provides a remarkable balance between computational cost and accuracy. DFT is applied in many areas including solid state physics where it was first implemented and used successfully for decades. The impact of DFT was recognized with the award of the 1998 Nobel prize in Chemistry to Walter Kohn for his development of the theory [4] and to John Pople [5] for his contributions to computational chemistry.

A particularly interesting and useful study that shows DFT's power of predictability is the successful discovery of a new, more efficient catalyst for the industrial production of ammonia [6].

There have been significant developments in the design of accurate functionals since the 1990s, which has led to DFT being at the forfront of more accurate methods being developed today. Time dependent DFT (TDDFT) is an extension to ground state DFT. Using TDDFT, people can treat the system with time dependent external potential. Also, TDDFT can provide more accurate results for some static properties, such as excitation energy and oscillation strength. My research has been motivated largely by how to apply DFT and TDDFT in solid-state physics and quantum chemistry problems. First I will briefly review traditional methods.

1.1 Wavefunction-based Methods

Every electronic system can be described by a wavefunction according to the Schrödinger equation (SE):

$$\hat{H}\Psi = E\Psi \tag{1.1}$$

where Ψ is the wavefunction for electrons and nuclei, E is the energy, and $\hat{H}$ is the Hamiltonian operator representing the total energy:

$$H = -\sum_i \frac{\hbar^2}{2m_e}\nabla_i^2 - \sum_A \frac{\hbar^2}{2m_A}\nabla_A^2 - \sum_i \sum_A \frac{e^2 Z_A}{|\mathbf{r}_i - \mathbf{r}_A|} + \sum_{i<j} \frac{e^2}{|\mathbf{r}_i - \mathbf{r}_j|} + \sum_{A<B} \frac{e^2 Z_A Z_B}{|\mathbf{r}_A - \mathbf{r}_B|} \tag{1.2}$$

m_e and m_A are the masses of the electrons and nuclei, respectively. $\mathbf{r}_a$ is the position of particles a; i, j run over electrons, and A, B run over the nuclei. The wavefunction, Ψ, is then a function of $3N$ coordinates, where N is the total number of electrons and nuclei. Unless otherwise stated, we shall henceforth use atomic units ($\hbar = e^2 = m_e = 1$), so that all energies are in Hartrees and all lengths in Bohr radii.

The ultimate goal of most quantum chemical and solid-state physics approaches is the approximated solution of the Schrödinger Equation. The motions of the particles are coupled and none move independently of the other. This presents a very complicated problem, making it impossible to solve exactly. For most systems, the problem can be simplified somewhat by making the Born-Oppenheimer (BO) approximation. Since the nuclei move on a much longer time scale than the electrons, one can ignore the kinetic energy of the nuclei when solving for the electrons, and treat an electronic Hamiltonian (the inter-nuclear repulsion also becomes a constant) for each point on a potential energy surface [7].

Even within the BO approximation, it is still hard to solve the electronic problem exactly for systems with more than one electron. Approximations must be made to the wavefunction.

The *variational principle* holds a very prominent place in all quantum chemical applications. The variational principle states that the energy computed as the expectation value of the Hamilton operator $\hat{H}$ from any guessed Ψ_{trial} will be an upper bound to the true energy of the ground state, i.e.,

$$\langle \Psi_{\text{trial}} | \hat{H} | \Psi_{\text{trial}} \rangle = E_{\text{trial}} \leq E_0 = \langle \Psi_0 | \hat{H} | \Psi_0 \rangle, \tag{1.3}$$

where the equality holds if and only if Ψ_{trial} is identical to Ψ_0.

Hartree developed a self-consistent field (SCF) method wherein one makes an initial guess of the wavefunctions of all occupied atomic orbitals (AOs) in a system [8]. These are then used to construct one electron hamiltonian operators which consist of the kinetic energy of the electrons, the electron-nuclear attraction potential, and an effective potential that approximates the electron-electron repulsion (the Hartree potential). Solving the SE with these one-electron hamiltonians then provides an updated set of wavefunctions and the procedure is repeated until there are no further changes in the updated wavefunctions up to a chosen

convergence. This method was extended to molecular systems by Roothaan.[9]

The Pauli exclusion principle states that the electronic wavefunction must be antisymmetric under exchange of any two particles in the system.[10] One clever and simple way to obtain a wavefunction that obeys this principle is to place single-electron orbitals inside a Slater determinant. Fock later extended Hartree's SCF method to Slater determinants. These so-called Hartree-Fock (HF) MOs are eigenfunctions of the set of one-electron hamiltonians. Although an improvement over Hartree's method, the HF wavefunction cannot be exact because of its restricted form as a Slater determinant. It contains exchange effects but completely neglects any electron correlation.

A first way to introduce correlation is through a perturbation approach. When one is dealing with a Slater determinant approximation, one may express the total energy of a system as the sum of a kinetic energy of electrons, electron-nuclear interaction energy, electron-electron repulsion energy, and exchange and correlation energies. Møller-Plesset Perturbation theory is defined by setting the exchange energy equal to the HF exchange energy and evaluating the correlation energy from perturbation theory with the HF hamiltonian as the zeroth order hamiltonian (Eqn. 1.4) [11, 12],

$$H = H^{(0)} + \lambda V \tag{1.4}$$

where $H^{(0)}$ is the HF hamiltonian, λ is a dimensionless parameter that changes in value from 0 to 1 and transforms $H^{(0)}$ into H, and V is a perturbing operator that represents the potential due to electron-electron repulsion not included in the HF potential. The method most frequently applied is perturbation up to second order of λ (MP2). Higher order MP theories are much more costly with very little improvement in accuracy.

A further extension is to consider all excitations from the HF determinant, called full configuration interaction (full CI). A full CI calculation with an infinite

basis is an exact solution to the non-relativistic, time-independent Schrödinger equation within the BO approximation. Although no reoptimization of HF orbitals is required, it is still extremely computationally demanding to consider all possible excitations for any reasonably sized system of more than 10 electrons [4]. One often considers a limited number of excitations to simplify the calculation. Most commonly used is CISD where only the complete set of single and double excitations are considered.

Another popular method is coupled cluster theory [13, 14]. This arises from expressing the full CI wavefunction as

$$\Psi = e^{T}\Psi_{HF} \tag{1.5}$$

$$T = T_1 + T_2 + ... + T_N \tag{1.6}$$

where T is the cluster operator, N is the number of electrons, and the T_i operators give all possible determinants that have i excitations. There are various levels of this, depending on how many excitations are included.

These correlation molecular orbital methods are computationally very costly and scale poorly with system size with the best one scaling as N^4, where N is the number of electrons. In the next section we consider a method that is not only often as accurate and reliable, but moreover is computationally less costly; this is particularly important for systems with large numbers of electrons.

1.2 Density Functional Theory

In the Schödinger equation, the external potential describes the interaction of the electrons with the nuclei or the external fields, determines the electronic properties of the system. Density functional theory (DFT) is a method in which all the properties will be calculated based on the ground state density. The Hohenberg-Kohn theorem [2] proves that once the electron-electron interaction is given, the

external potential will be uniquely determined by the ground state electronic density; thus, the wavefunctions and all other components can be solved from the density. This is the foundation of Density Functional Theory. In DFT, rather than having to solve the highly-coupled Schödinger equation for the many-body wavefunction one needs only to determine the ground state electronic density of the system.

Since the density is the only thing we need to know in DFT, we can imagine a non-interacting system, which has same density as the fully interacting physical system, and solve the density from the non-interacting system. Such a non-interacting system is known as the Kohn-Sham (KS) system. In the KS system, there is no coulomb interacting terms, so it can be easily decoupled. The result is a set of one-body electron equations (KS equations) which are far simpler to solve than the highly correlated Schrödinger equation:

$$\left\{-\frac{1}{2}{\nabla_i}^2 + v_{\mathrm{S}}[n](r)\right\}\phi_i = \epsilon_i\phi_i. \tag{1.7}$$

The solutions of KS equations is the orbitals of KS system, and the density of KS system is the summation of the density of the lowest N orbitals,

$$n(\mathbf{r}) = \sum_{i=1}^{N} |\phi_i(r)|^2. \tag{1.8}$$

In the KS equation Eq. (1.7), the electronic Hamiltonian operator consists of kinetic and KS potential contributions, and the Kohn-Sham potential v_{S}, is composed of a Hartree potential (v_{H}), the external potential (v_{ext}), and all that remains is lumped into what is called the exchange-correlation potential (v_{XC}).

$$v_{\mathrm{S}}(\mathbf{r}) = v_{\mathrm{H}}(\mathbf{r}) + v_{\mathrm{ext}}(\mathbf{r}) + v_{\mathrm{XC}}(\mathbf{r}). \tag{1.9}$$

The Hartree potential is given by

$$v_{\mathrm{H}}(\mathbf{r}) = \int d^3r' \frac{n(\mathbf{r}')}{|\mathbf{r} - \mathbf{r}'|}, \tag{1.10}$$

and describes the electrostatic repulsion of the electrons. The external potential is the same as the fully interacting physical system, it expresses the attraction between the nuclei and the electrons and any external field that may be present. In principle, the exchange-correlation potential v_{XC} is a functional of the ground state density n, and if the exact v_{XC} were known, the KS method would provide the exact properties (energies, etc.) of the interacting systems. And can be sovled exactly, but in practice, v_{XC} must be approximated.

The KS potential v_{S} is a functional of density n, but n is the sum of the KS obitals, so the KS equation Eq. (1.7) is a self consistent equation. We can use iteration methods to find the solutions.

After we get the electronic density, which is the same for the non-interacting and interacting system, the ground state energy of the interacting system can be expressed as a sum of functionals of the density:

$$E[n] = T_{\mathrm{S}}[n] + \int d^3\mathbf{r} n(\mathbf{r}) v_{\mathrm{ext}}(\mathbf{r}) + U[n] + E_{\mathrm{XC}}[n]. \tag{1.11}$$

T_{S} is the kinetic energy of the KS system. It is calculated from the KS orbitals and is not the same kinetic energy T of the real system:

$$T_{\mathrm{S}} = -\frac{1}{2}\sum_{i=1}^{N} \nabla_i^2 \phi_i(\mathbf{r}). \tag{1.12}$$

The hartree energy

$$U[n] = \frac{1}{2}\int d^3\mathbf{r} \int d^3\mathbf{r}' \frac{n(\mathbf{r})n(\mathbf{r}')}{|\mathbf{r}-\mathbf{r}'|} \tag{1.13}$$

The exact exchange energy can be obtained from the orbitals, but most of the approximations deal with the exchange and correlations energies together since they often have different signs of error in the approximation so their errors can be partly canceled.

The exchange-correlation potential v_{XC} is the functional derivative of the exchange correlation energy with respect to the density n:

$$v_{\mathrm{XC}}(\mathbf{r}) = \frac{\delta E_{\mathrm{XC}}}{\delta n(\mathbf{r})} \tag{1.14}$$

We must note that the density functional theory itself is an exact theory if the functional dependence of $v_{\mathrm{XC}}[n]$ are known, but in practice, we always need approximation for the exchange-correlation part. The present approximate functionals can be local, semi-local, and non-local.

The exact $v_{\mathrm{XC}}[n](\mathbf{r})$ depends on the density n all over the space, but we can make a simple assumption that the exchange-correlation potential only depends on the density at this point and contains no information about neighboring points. This approximation is called local density approximation (LDA).

$$v_{\mathrm{XC}}^{\mathrm{LDA}}[n](\mathbf{r}) = v_{\mathrm{XC}}[n(\mathbf{r})]. \tag{1.15}$$

LDA is first introduced by [3], and widely used in DFT calculations, such as SVWN5 in GAUSSIAN code [15, 16]. The parameters are chosen to make the functional exact for uniform gas. In most of the cases, LDA functional works remarkably well despite its simplicity and is extensively used in solid state physics, one of the largest fields where DFT is applied.

Semi-local functionals are an improvement of local approximation. They depend on not only the density at a certain point, but also the gradient of the density at that point. So for the electrons in rapidly changing external potential, semi-local functionals give better approximations than the local approximation. One example of semi-local approximation is the generalized gradient approximation (GGAs). The most popular GGAs in quantum chemistry are the PW91 [17] and PBE [18] functionals which are also often used in solid state physics.

The approximated functionals mentioned above are non-empirical. There are also some empirical functionals, in such approximation, some parameters must be fitted for a particular system. Some hybrid approximations are also used, where one approximation is used for exchange potential while another approximation is applied to the correlation part.

1.3 Time Dependent Density Functional Theory

DFT is very successful to solve the ground state properties of electrons in time-independents potentials. But since the density we used in DFT is the ground state density, so the excitation problems can not be solved by DFT method, also, when the system has a time-dependent potential, we need to extend DFT in order to solve it. Time-dependent density functional theory (TDDFT) is such a extension of DFT.

As Hohenberg-Korn theorem to DFT, Runge-Gross theorem [19] is the fundamental theory of TDDFT. It is proved that there is also a one to one correspondence between time-dependent density $n(\mathbf{r}t)$ and time-dependent potential $v_{\text{ext}}(\mathbf{r}t)$ for a given initial state.

So we can define a fictious system of non-interaction electrons that satisfy time-dependent Kohn-Sham equations

$$i\dot{\phi}_j(\mathbf{r}t) = \left(-\frac{\nabla^2}{2} + v_{\text{S}}[n](\mathbf{r}t)\right)\phi_j(\mathbf{r}t), \tag{1.16}$$

where the density is

$$n(\mathbf{r}t) = \sum_{j=1}^{N} |\phi_j(\mathbf{r}t)|^2. \tag{1.17}$$

The Kohn-Sham potential $v_{\text{S}}(\mathbf{r}t)$ has three parts

$$v_{\text{S}}(\mathbf{r}t) = v_{\text{ext}}(\mathbf{r}t) + v_{\text{H}}(\mathbf{r}t) + v_{\text{XC}}(\mathbf{r}t). \tag{1.18}$$

The exchange-correlation potential is a functional of the entire history of the density $n(\mathbf{r}t)$, the initial interacting wavefunction $\Psi(0)$ and the initial Kohn-Sham wavefunction $\Phi(0)$, but in most of the TDDFT calculation, the adiabatic approximation is used, in such approximation, v_{XC} is only a functional of the present density

$$v_{\text{XC}}[n;\Psi(0),\Phi(0)](\mathbf{r}t) = v_{\text{XC}}^{\text{adia}}[n(t)](\mathbf{r}). \tag{1.19}$$

So it approximates the functional as being local in time. When the time-dependent external potential changes very slow, the adiabatic approximation will be valid.

In practice, the spatial locality of the functional is also approximated, this adiabatic local density approximation (ALDA) is always used in the TDDFT calculations.

Although TDDFT is a method designed for the system with a time-dependent external potential, it also can be used as a improvement to ground state DFT, to compute the static properties of atoms and molecules, such as transition frequencies and oscillation strength.

In many cases, we are only interested in the response to a weak change in potential $\delta v_{\text{ext}}(rt)$, so linear response is used, i.e. we want to know what is the first order perturbation. In TDDFT, the density plays the most important role, so we need to know how density responses to the perturbation. We define the susceptibility $\chi[n_0](\mathbf{r},\mathbf{r}';t-t')$ as the response of the ground state density to a small change in the external potential:

$$\delta n(\mathbf{r}t) = \int dt' \int d^3r' \chi[n_0](\mathbf{r},\mathbf{r}';t-t')\delta v_{\text{ext}}(\mathbf{r}'t'), \tag{1.20}$$

and that χ contains most of what we want to know about the response of a system. In Lehman representation, χ can be written as

$$\chi(\mathbf{r},\mathbf{r}';\omega) = \sum_I \frac{n_{0I}(\mathbf{r})n^*_{0I}(\mathbf{r}')}{\omega+(E_I-E_0)+i0^+} + c.c.(\omega\to-\omega), \tag{1.21}$$

where I spans over all the excited states and

$$n_{jk} =< j|\hat{n}(\mathbf{r})|k> . \tag{1.22}$$

When the perturbing field is weak, perturbation theory applies. Then we only need to know the knowledge of v_{XC} in the vicinity of the initial state, which we take to be a non-degenerate ground state. Writing $n(\mathbf{r}t) = n(\mathbf{r}) + \delta n(\mathbf{r}t)$, we have

$$v_{\text{XC}}[n+\delta n](\mathbf{r}t) = v_{\text{XC}}[n](\mathbf{r}) + \int dt' \int d^3r' f_{\text{XC}}[n](\mathbf{r}\mathbf{r}',t-t')\delta n(\mathbf{r}'t'), \tag{1.23}$$

where f_{XC} is the exchange-correlation kernel,

$$f_{\text{XC}}[n](\mathbf{r}\mathbf{r}',t-t') = \frac{\delta v_{\text{XC}}(\mathbf{r}t)}{\delta n(\mathbf{r}'t')}. \tag{1.24}$$

The exchange-correlation kernel is time-dependent, but in practice, the adiabatic approximation is always used in linear response, so the kernel has the form:

$$f_{\mathrm{XC}}^{\mathrm{adia}}(\mathbf{r}\mathbf{r}', t-t') = \left.\frac{\delta v_{\mathrm{XC}}^{\mathrm{gs}}[n_0](\mathbf{r})}{\delta n_0(\mathbf{r})}\right|_{n_0(\mathbf{r})=n(\mathbf{r}t)} \delta(t-t'). \tag{1.25}$$

In the non-interacting Kohn-Sham system, we can also define its susceptibility χ_{S}, which says how the density response to the change of KS potential $\delta v_{\mathrm{S}}(\mathbf{r}t)$. The interacting real system and non-interacting Kohn-Sham system are quit different, but since they yield same density, and the density also determine the potential once the electron interaction and initial state are given, we can use the exchange-correlation kernel link them. We then get a Dyson-like response equation

$$\chi(\mathbf{r}\mathbf{r}';\omega) = \chi_{\mathrm{S}}(\mathbf{r}\mathbf{r}';\omega) + \int d^3r_1 \int d^3r_2 \chi_{\mathrm{S}}(\mathbf{r}\mathbf{r}_1;\omega)\left(\frac{1}{|\mathbf{r}_1-\mathbf{r}_2|} + f_{\mathrm{XC}}(\mathbf{r}_1\mathbf{r}_2;\omega)\right)\chi(\mathbf{r}_2\mathbf{r}';\omega). \tag{1.26}$$

This is the key equation of TDDFT linear response. After we obtain χ_{S} from the KS system, we can solve χ from Eq. (1.26).

The excitations lies at the poles of χ, so if we only want to get the transition frequencies, instead of solving the whole χ, we just need to know how find the poles of χ. Casida shows that [20], finding the poles of χ is equivalent to solving the eigenvalue problem:

$$\sum_{q'} \tilde{\Omega}_{qq'}(\omega) v_{q'} = \Omega v_{q'}, \tag{1.27}$$

where q is a double index, representing a transition from occupied KS orbital i to unoccupied KS orbital a, $\omega_q = \epsilon_a - \epsilon_i$ is the KS transition frequency, and $\Omega = \omega^2$ is the square of the true transition frequency. The matrix element

$$\tilde{\Omega}_{qq'} = \delta_{qq'}\omega_q^2 + 2\sqrt{\omega_q\omega_{q'}} \int d^3r \int d^3r' \Phi_q^*(\mathbf{r}) f_{\mathrm{HXC}}(\mathbf{r}\mathbf{r}';\omega)\Phi_{q'}(\mathbf{r}'). \tag{1.28}$$

where $\Phi_q(\mathbf{r}) = \phi_i^*(\mathbf{r})\phi_a(r)$, and $f_{\mathrm{HXC}}(\mathbf{r}\mathbf{r}';\omega) = 1/|\mathbf{r}-\mathbf{r}'| + f_{\mathrm{XC}}(\mathbf{r}\mathbf{r}';\omega)$ is the Hartree-exchange-correlation kernel. The matrix elements have dependence on ω, so we can use iteration methods to get the self-consistent solution ω, but in the adabatic approximation, it becomes a normal matrix eigenvalue problem.

Some other approximations can be applied to the matrix formula, such as truncating the matrix, only keeping the low excitations, or assuming the coupling between orbitals are weak, so we can ignore the off-diagonal matrix elements.

Chapter 2
A Toy Model and the TDDFT View on It

To show how TDDFT works, we apply it on a toy model, and in the later chapters, we will continue use this model to demonstrate our methods.

The toy model contains two one dimensional fermions, they are bonded in a parabolic well, and the interaction between them is a δ-function repulsion of strength λ. The Hamiltonian of the system is

$$\hat{H} = -\frac{1}{2m}\left(\frac{d^2}{dx_1^2} + \frac{d^2}{dx_2^2}\right) + \frac{1}{2}k(x_1^2 + x_2^2) + \lambda\delta(x_1 - x_2). \tag{2.1}$$

To make the calculation simple, we take $m = k = 1$, and leave λ as the only argument.

2.1 Exact Solution

The toy model can be solved exactly. First, we transform it to center of mass and relative coordinates

$$R = \frac{x_1 + x_2}{2}, \quad u = x_1 - x_2, \tag{2.2}$$

the Schrödinger equation will decouple into two separate equations. The one in center of mass coordinate,

$$-\frac{1}{4}\frac{d^2}{dR^2}\Phi^R(R) + R^2\Phi^R(R) = E^R\Phi^R(R), \tag{2.3}$$

is a simple harmonic oscillator. And the other one in relative coordinate is

$$-\frac{d^2}{du^2}\phi^u(u) + \frac{1}{4}u^2\phi^u(u) + \lambda\delta(u)\phi^u(u) = E^u\phi^u(u). \tag{2.4}$$

In this section, we will give a exact solution to Eq. (2.4).

The Hamiltonian is

$$\hat{H} = -\frac{d^2}{du^2} + \frac{1}{4}u^2 + \lambda\delta(u), \tag{2.5}$$

the odd solutions $\phi^u(-u) = -\phi^u(u)$ satisfy $\phi^u(0) = 0$, thus the δ function has no effect on it, the solution is the same as the odd solution of the simple harmonic oscillator. So we only look at the even solution $\phi^u(-u) = \phi^u(u)$, when $u > 0$, the Schrödinger Equation is

$$-\frac{d^2}{du^2}\phi^u(u) + \frac{1}{4}u^2\phi^u(u) - E^u\phi^u(u) = 0, \tag{2.6}$$

and the boundary condition is

$$\left.\frac{d\phi^u(u)}{du}\right|_{u=0+} = \frac{\lambda}{2}\phi^u(0). \tag{2.7}$$

Take

$$\phi^u(u) = \psi(u)\exp(-u^2/4), \tag{2.8}$$

then

$$-\frac{d^2}{du^2}\psi(u) + u\frac{d}{du}\psi(u) - (E^u - \frac{1}{2})\psi(u) = 0, \tag{2.9}$$

and

$$\left.\frac{d}{du}\psi(u)\right|_{u=0} = \frac{\lambda}{2}\psi(0). \tag{2.10}$$

Change the variable to $w = u^2/2$, we have

$$\frac{d}{du}\psi(u) = \sqrt{2w}\frac{d}{dw}\psi(w), \tag{2.11}$$

$$\frac{d^2}{du^2}\psi(u) = \frac{d}{dw}\psi(w) + 2w\frac{d^2}{dw^2}\psi(w) \tag{2.12}$$

thus

$$w\frac{d^2}{dw^2}\psi(w) + (\frac{1}{2} - w)\frac{d}{dw}\psi(w) - \frac{1 - 2E^u}{4}\psi(w) = 0, \tag{2.13}$$

this is the Kummer's Equation with $a = (1-2E^u)/4$ and $b = 1/2$. The boundary condition will become

$$\left.\sqrt{2w}\frac{d}{dw}\psi(w)\right|_{w=0} = \frac{\lambda}{2}\psi(0) \tag{2.14}$$

The solution of Kummer's Equation are

$$M(a,b,w) = 1 + \frac{aw}{b} + \frac{(a)_2 w^2}{(b)_2 2!} + \cdots + \frac{(a)_n w^2}{(b)_n 2!} + \cdots, \tag{2.15}$$

where

$$(a)_n = a(a+1)(a+2)\cdots(a+n-1),\ (a)_0 = 1, \tag{2.16}$$

and

$$N(a,b,w) = w^{1-b} M(1+a-b, 2-b, w); \tag{2.17}$$

The complete solution is

$$\psi(w) = AM(\frac{1-2E^u}{4}, \frac{1}{2}, w) + BN(\frac{1-2E^u}{4}, \frac{1}{2}, w) \tag{2.18}$$

where A and B are arbitrary constants. Using the boundary condition

$$\psi(0) = A, \quad \sqrt{2w}\frac{d}{dw}\psi(w)\Big|_{w=0} = \frac{B}{\sqrt{2}} \tag{2.19}$$

we can relate A and B as

$$B = \frac{A}{\sqrt{2}}\lambda. \tag{2.20}$$

As $|w| \to \infty$,

$$M(a,b,w) = \frac{\Gamma(b)}{\Gamma(a)} e^w w^{a-b}[1 + O(|w|^{-1})], \quad (\Re w > 0) \tag{2.21}$$

$$\begin{aligned}
\psi(w) &= A\frac{\Gamma(\frac{1}{2})}{\Gamma(\frac{1-2E^u}{4})} e^w w^{\frac{-1-2E^u}{4}}[1 + O(|w|^{-1})] \\
&\quad + B\frac{\Gamma(\frac{3}{2})}{\Gamma(\frac{3-2E^u}{4})} e^w w^{\frac{-1-2E^u}{4}}[1 + O(|w|^{-1})] \\
&= A\left(\frac{\Gamma(\frac{1}{2})}{\Gamma(\frac{1-2E^u}{4})} + \frac{\lambda}{\sqrt{2}}\frac{\Gamma(\frac{3}{2})}{\Gamma(\frac{3-2E^u}{4})}\right) \\
&\quad \times e^w w^{\frac{-1-2E^u}{4}}[1 + O(|w|^{-1})]
\end{aligned} \tag{2.22}$$

The bound state requires $\psi(w)$ goes to ∞ slower than $\exp(w/2)$, so

$$\begin{aligned}
\lambda &= -\frac{\sqrt{2}\Gamma(\frac{1}{2})\Gamma(\frac{3-2E^u}{4})}{\Gamma(\frac{1-2E^u}{4})\Gamma(\frac{3}{2})} \\
&= -\frac{2\sqrt{2}\Gamma(\frac{3-2E^u}{4})}{\Gamma(\frac{1-2E^u}{4})}
\end{aligned} \tag{2.23}$$

The exact wavefunction is hard to compute, so in practice, we use the shooting method to solve the relative coordinate part numerically. The wavefunction in both the center of mass and the relative coordinate can be taken as real functions.

In the toy model, we use a pair of number $[J, j]$ to notate the levels of the system, where J and j are the quantum numbers in the center of mass and relative coordinates eigenstates respectively. We are only interested in the singlet states of the system, so the solution $\phi(u)$ must be an even function, thus j is even. So the possible values of J and j are $J = 0, 1, 2, \ldots$ and $j = 0, 2, 4, \ldots$. For example, the ground state is $[0, 0]$ and the first five excited states are $[1, 0]$, $[0, 2]$, $[2, 0]$, $[1, 2]$, and $[3, 0]$.

2.2 Exact Kohn-Sham System

The exact KS system is the non-interacting system that has the same ground state density as the interacting system. Generally, the KS system can not be obtained exactly, but for the toy model, the ground state density can be calculated as

$$\begin{aligned} n(x) &= \int dx_1 |\Psi_0(x, x_1)|^2 \\ &= \int dx_1 |\Phi_0^R(\frac{x + x_1}{2})\phi_0^u(x - x_1)|^2. \end{aligned} \tag{2.24}$$

As we know, the KS system also has the same density, and the ground state of the KS system has both the two electrons on the lowest orbital ϕ_0, so

$$n(x) = 2|\phi_0(x)|^2. \tag{2.25}$$

We take the ground state orbital in the KS system as a positive function. Since the density is known, the ground state orbital is

$$\phi_0(x) = \sqrt{\frac{n(x)}{2}}. \tag{2.26}$$

The KS system satisfies

$$\left\{ -\frac{1}{2}\frac{d^2}{dx^2} + v_{\mathrm{s}}(x) \right\} \phi(x) = \epsilon\phi(x), \tag{2.27}$$

so the KS potential $v_{\rm S}(x)$ can be determined if $\phi_0(x)$ is known,

$$v_{\rm S}(x) = \frac{\phi_0''(x)}{2\phi_0(x)} + c, \tag{2.28}$$

where c is a constant, we choose c such that when x is very large, the KS system will become the external potential $x^2/2$.

Next, we put the exact KS potential $v_{\rm S}(x)$ back to Eq. (2.27), then all the orbitals of the KS system can be solved exactly.

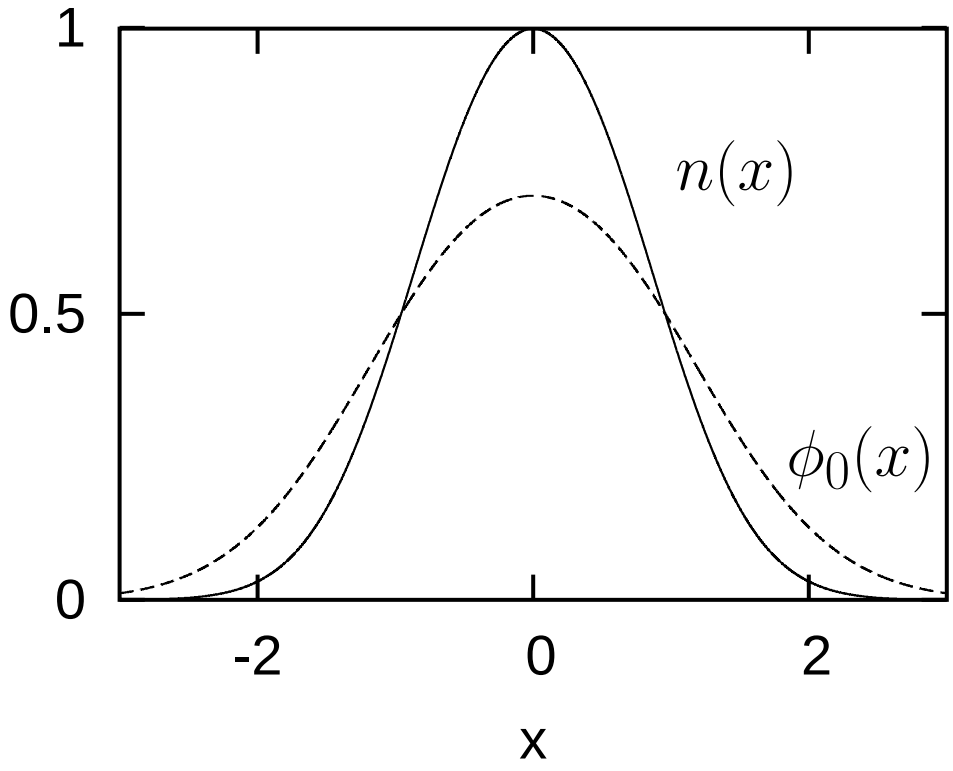

Figure 2.1: Exact density of the toy model (solid line) and the exact ground state orbital of the Kohn-Sham system (dashed line). The units used here are a.u..

In Fig. 2.1, we plot the exact density of the toy model with $\lambda = 1$, and the lowest orbital of the KS system, both of them are numerically exact. And in Fig. 2.2, the exact KS potential and the real external potential for the toy model. From this figure, we can see that when $x \to \infty$, the KS potential and the external potential are identical, but when x is small, there is a bump around $x = 0$, this is because in the interacting system, the contact repulsion makes the two electrons

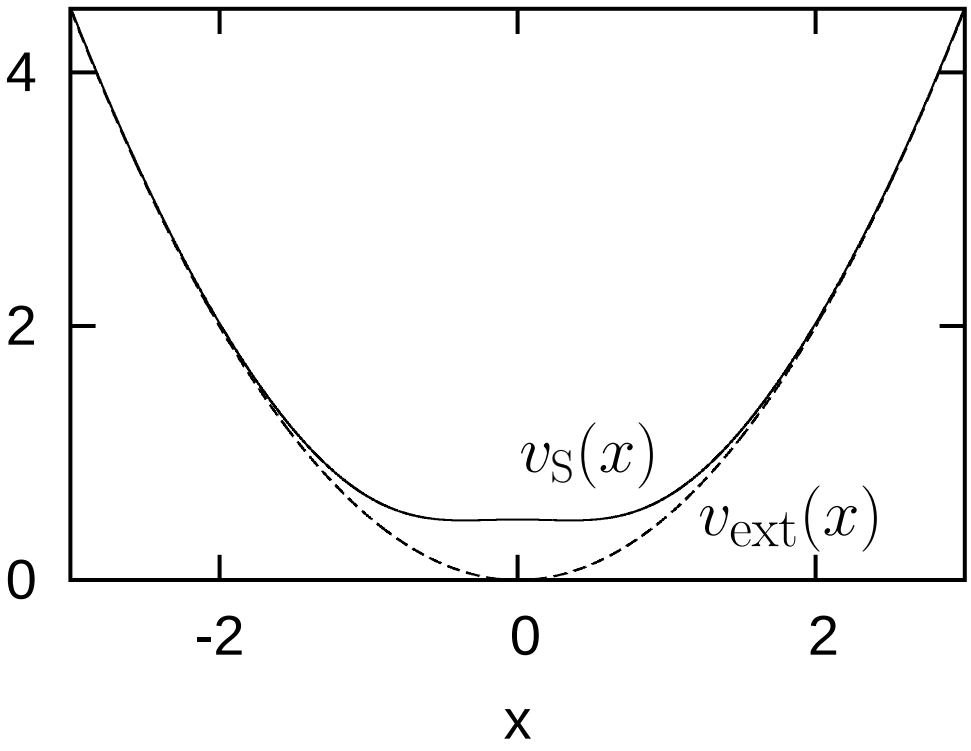

Figure 2.2: Exact KS potential of the toy model (solid line) and the exact external potential(dashed line). The units used here are a.u..

not able to both stay at $x = 0$, so the non-interacting system need a high KS potential here to have the same ground state density.

2.3 TDDFT on Excitations

The KS excitations are the energy different between the excited states and the ground state. Since the KS system only has the same ground state density as the real system, it can not give correct excitation information from its excited orbitals. Even for the ground state, the total energy of the orbitals are not the true ground state energy.

For the KS system of the toy model, the orbitals are the solutions to Eq. (2.27). Suppose the ground state orbital is $\phi_0(x)$, with energy ϵ_o, and the excitation are $\phi_1(x)$, $\phi_2(x)$, $\phi_3(x)$, and so on, with energies of ϵ_1, ϵ_2, and ϵ_3. So the singlet states

are:

$$\begin{aligned}
\Phi_{(0,0)}(x_1,x_2) &= \phi_0(x_1)\phi_0(x_2), \quad \text{ground state,} \\
\Phi_{(0,1)}(x_1,x_2) &= \frac{1}{\sqrt{2}}[\phi_0(x_1)\phi_1(x_2)+\phi_1(x_1)\phi_0(x_2)], \quad \text{first excited state,} \\
\Phi_{(1,1)}(x_1,x_2) &= \phi_1(x_1)\phi_1(x_2), \quad \text{second excited state,} \\
\Phi_{(0,2)}(x_1,x_2) &= \frac{1}{\sqrt{2}}[\phi_0(x_1)\phi_2(x_2)+\phi_2(x_1)\phi_0(x_2)], \quad \text{third excited state,} \\
&\cdots
\end{aligned}$$

The energies of the KS system are the summation of the orbital energies, so

$$\begin{aligned}
E_{(0,0)} &= 2\epsilon_0, \\
E_{(0,1)} &= \epsilon_0+\epsilon_1, \\
E_{(1,1)} &= 2\epsilon_0, \\
E_{(0,2)} &= \epsilon_0+\epsilon_2.
\end{aligned}$$

Thus the KS transition frequencies are

$$\begin{aligned}
\omega_{(0,1)} &= \epsilon_1-\epsilon_0, \\
\omega_{(1,1)} &= 2(\epsilon_1-\epsilon_0), \\
\omega_{(0,2)} &= \epsilon_2-\epsilon_0.
\end{aligned}$$

And we can see that $(0,1)$ and $(0,2)$ are single excitations and $(1,1)$ is a double excitation since both of the two electrons are excited from ground state to the first excited state.

In Fig. 2.3, the lowest several singlet states energies of the interacting system and the KS system are plotted. Please notice the notation of the levels are different. Although their energy level structures are similar, the KS energies are not good approximations to the real energy.

Now, we use TDDFT linear response calculate the excitations. When λ is small, the excitations are well separated, so the single pole approximation (SPA)

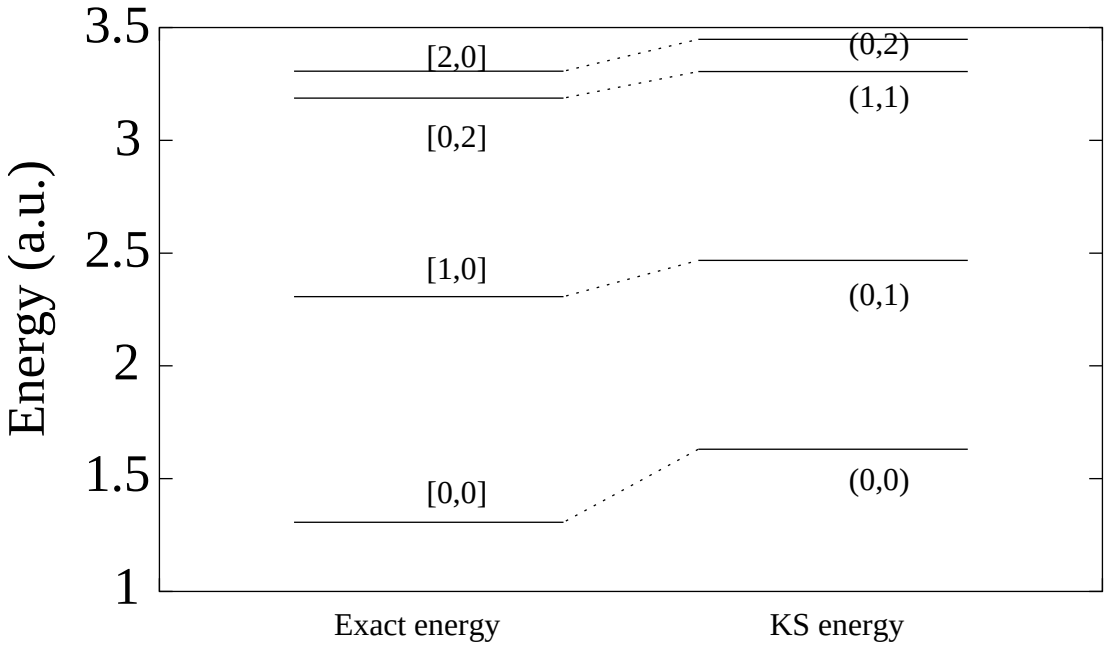

Figure 2.3: Exact Energies and KS energies of the singlet states of the toy model with $\lambda = 1$. The units used here are a.u..

is a good approximation to it. The formula we use here is

$$\omega = \omega_q + 2[q|f_{\text{HXC}}(\omega)|q] \tag{2.29}$$

Another approximation we will use is the adiabatic approximation for the kernel f_{HXC}, so f_{HXC} is frequency-independent. And we know that f_{X} is of the order of λ and f_{C} is of the order of λ^2, so when λ is small, f_{C} can be ignored. And for the two electron system, the exchange potential cancels half of the Hartree potential, so the kernel will become

$$f^A_{\text{HXC}} \approx f_{\text{HX}} = \frac{1}{2} f_{\text{H}} = \frac{\lambda}{2}\delta(x_1 - x_2). \tag{2.30}$$

Applying this to the toy model, q is an excitation from the only occupied orbital ϕ_0 to some unoccupied orbital ϕ_a, so for the excited state $(0, a)$ in the KS system, the transition frequency is

$$\begin{aligned} \omega &= \epsilon_a - \epsilon_0 + \lambda \int dx dx' \phi_0^*(x)\phi_a(x)\delta(x - x')\phi_0(x')\phi_a^*(x') \\ &= \epsilon_a - \epsilon_0 + \lambda \int dx |\phi_0^*(x)\phi_a(x)|^2. \end{aligned} \tag{2.31}$$

In Table 2.1, the numerical results of the excitation of the toy model are listed. The SPA improves the KS excitations to give more accurate results.

Table 2.1: Transition frequencies of the toy model with $\lambda = 0.2$ and an approximations from KS excitations and SPA results. The units used here are a.u..

True	KS	SPA
1.00000	0.9616	1.0014
2.00000	1.9532	1.9833
3.00000	2.9483	2.9734

One important thing about Eq. (2.31) is that this formula can only be used to calculate the excitation from $(0, 0)$ to $(0, a)$ (single excitation), but not the excitation from $(0, 0)$ to (a, a') (double excitation). In Chapter 3, we will discuss how to treat double excitions in TDDFT.

Chapter 3
Double Excitations in TDDFT

Ground-state density functional theory (DFT) is an efficient and popular calculation method in solid-state physics and quantum chemistry [2, 3]. The one-to-one mapping between densities and potentials gives rise to a Kohn-Sham (KS) system of non-interacting electrons, whose equations are must faster to solve than the fully interacting Schrödinger equation. All the ground-state properties of the system can be obtained, in principle exactly, via DFT [49, 4]. In practice, approximations must be made for the unknown exchange-correlation energy, and recent years have seen the development of increasingly accurate functionals [18], applied to increasingly complex systems.

Time-dependent DFT (TDDFT) is an extension of the ground-state theory to time-dependent potentials [19]. Today this is most widely used in the linear response regime, where excitations and oscillator strengths of atoms, molecules and solids are calculated (see for example [50] for many references). In principle, all excitations of the system may be obtained exactly from those of the KS system together with the Hartree-exchange-correlation kernel through an integral equation [51, 20]:

$$\chi(\mathbf{r},\mathbf{r}';\omega) = \chi_{\mathrm{S}}(\mathbf{r},\mathbf{r}';\omega) + \int d^3r_1 \int d^3r_2 \chi_{\mathrm{S}}(\mathbf{r},\mathbf{r}_1;\omega) \times f_{\mathrm{HXC}}(\mathbf{r}_1,\mathbf{r}_2;\omega)\chi_{\mathrm{S}}(\mathbf{r}_2,\mathbf{r}';\omega). \tag{3.1}$$

where the density-density response function, or susceptibility $\chi(\mathbf{r},\mathbf{r},\omega)$ contains poles at all the excitations of the true system. Oscillator strengths may be obtained from the residues. The Dyson-like equation Eq. (3.1) enables us to obtain

these from the KS susceptibility $\chi_{\rm S}(\mathbf{r},\mathbf{r}',\omega)$ and $f_{\rm HXC}[n_0](\mathbf{r},\mathbf{r}',\omega) = 1/|\mathbf{r}-\mathbf{r}'| + f_{\rm XC}(\mathbf{r},\mathbf{r}',\omega)$, the sum of the Hartree and exchange-correlation kernel. Almost always an adiabatic approximation for the latter is used, in which the kernel is frequency-independent; most often it is simply the functional derivative of the ground-state exchange-correlation potential from which the bare KS transitions of the KS susceptibility were calculated. This has been cast in matrix form [20], programmed in many quantum chemistry codes such as Gaussian, and given rise to thousands of calculations of excitations. In many cases, but not all, the transition frequencies are remarkably accurate, even when those states have significant double-excitation character.

On the one hand, the exact TDDFT formalism should in principle produce transitions to excitations of any number, but on the other hand, the integral (or matrix) equations are essentially corrections to the KS response, which contains poles at only single excitations. How are the "extra" poles of the true system generated in the formalism? In what sense do the present adiabatic calculations capture states of double-excitation character? We will answer these questions. We will show that the exact exchange-correlation kernel has a very strong frequency-dependence in the region near double(multiple)-excitations and that it is this that enables TDDFT to generate more poles and produce the double excitations. By studying a simple model, two interacting fermions in a one-dimensional harmonic well interacting via a delta-function repulsion, we show exactly what this frequency-dependent behavior is. Furthermore, motivated by techniques from wavefunction CI theory, we deduce an approximate model for $f_{\rm XC}(\omega)$ within a generalized single pole approximation, applicable for a general system where a double excitation is coupled with a single excitation. We also want to give some explanations about how present adiabatic TDDFT calculations get states of double-excitations.

We begin by showing that an adiabatic xc kernel is unable to produce multiple

excitations.

The susceptibility may be written in Lehman representation as

$$\chi(\mathbf{r},\mathbf{r}';\omega) = \sum_I \left\{ \frac{f_I(\mathbf{r}) f_I^*(\mathbf{r}')}{\omega - \omega_I + i0^+} - \frac{f_I^*(\mathbf{r}) f_I(\mathbf{r}')}{\omega + \omega_I + i0^+} \right\}, \tag{3.2}$$

with

$$f_I(\mathbf{r}) = < 0|\hat{n}(\mathbf{r})|I > . \tag{3.3}$$

where I labels all the excited states and ω_I is their transition frequency. This expression also holds for the KS susceptibility where the excited-states are excited Slater determinants and the transition frequencies are orbital energy differences. Due to the one-body nature of the density operator in the numerator, only single-excitations contribute to the KS susceptibility, but this is not true for the interacting system where exact eigenstates are in general mixtures of single, double, and maybe higher excitations. The true susceptibility contains poles at states dominated by any number of excitations: $\chi_{\rm S}$ has fewer poles than χ. A frequency-independent xc kernel, $f_{\rm XC}(\mathbf{r},\mathbf{r}',\omega) = f_{\rm XC}(\mathbf{r},\mathbf{r}')$, such as in ALDA, in the linear response equation Eq. (3.1) can not generate more poles, and so the multiple excitations are lost.

The failure of an adiabatic approximation to produce doubles is also readily seen in Casida's matrix formulation [20]. Here, the squares of the true transition frequencies $\Omega_I = \omega_I^2$ are the (generalized) eigenvalues of the equation

$$\sum_{q'} \widetilde{\Omega}_{qq'}(\omega) v_{q'} = \Omega v_q, \tag{3.4}$$

with

$$\widetilde{\Omega}_{qq'} = \delta_{qq'}\Omega_q + 4\sqrt{\omega_q \omega_{q'}} < q|f_{\rm HXC}(\omega)|q' >, \tag{3.5}$$

and

$$\Phi_q(\mathbf{r}) = \phi_i^*(\mathbf{r})\phi_a(\mathbf{r}). \tag{3.6}$$

Here q is a double index, representing a single excitation: a transition from an occupied KS orbital ϕ_i to an unoccupied one ϕ_a. The KS transition frequency is the difference in the KS orbital energies, $\omega_q = \epsilon_a - \epsilon_i$.

Because the matrix in Eq.(3.4) spans only the KS single-excitations, it is clear that if f_{HXC} is frequency-independent, thus the number of eigenvalues of the matrix is only equal to the number of single excitations. Multiple excitations can not be gained from the matrix.

A zeroth-order approximation for the true transition frequencies is obtained from expanding the linear response equation around each KS transition frequency [51], assuming each is well-separated. This "single-pole approximation" (SPA) can also be derived from neglecting the off-diagonal terms in Casida's matrix and assuming the correction due to f_{HXC} is small compared with the bare Kohn-Sham value. One finds

$$\omega = \omega_q + 2 < q|f_{\text{HXC}}|q > \tag{3.7}$$

The SPA thus corrects the single excitations of the KS system towards the true ones. Compared with the difference between the unoccupied and occupied KS orbitals, ALDA gives us better results of the transition frequency [52], but when using a frequency-independent f_{XC}, we will lose the multiple excitations.

Here we will use a simple model to show explicitly how the double excitations are missing and how can we find them by using a frequency-dependent f_{XC}. Our system contains two 1-dimensional fermions in a parabolic external potential, interacting via a delta-function repulsion of strength λ. The Hamiltonian of the system is

$$\hat{H} = -\frac{1}{2}(\frac{d^2}{dx_1^2} + \frac{d^2}{dx_2^2}) + \frac{1}{2}\omega^2(x_1^2 + x_2^2) + \lambda\delta(x_1 - x_2). \tag{3.8}$$

Transforming to center of mass and relative coordinates

$$R = \frac{x_1 + x_2}{2}, \quad u = x_1 - x_2, \tag{3.9}$$

the Schrödinger Equation can be easily decoupled: the center of mass part is just a harmonic oscillator, and the relative coordinates part can be solved numerically. For the singlet states, the quantum number of the relative coordinate are even, so we have only one level $(1, 0)$ for the first excited state, whose center of mass part

is on the first excited state while the reletive coordinates part is on the ground state; and we have two levels $(2,0)$ and $(0,2)$ for the second excited states. After calculating the exact ground state density, we can find the exact KS potential, and solve for all the KS orbitals. In Table 1, we list the true transition frequencies of the first two singlet excited states, KS orbital energy differences, and those from the single pole approximation, for a weak interaction ($\lambda = 0.1$). Because λ is small, in the SPA calculation, we have neglected the correlation in $f_{\rm XC}$: $f_{\rm X}$ is of the order of λ, but $f_{\rm C}$ is of the order of λ^2. So in this case,

$$f_{\rm HXC} \approx f_{\rm HX} = \frac{1}{2} f_{\rm H} = \frac{\lambda}{2}\delta(x_1 - x_2). \tag{3.10}$$

Further, we expand SPA using this kernel $f_{\rm HX}$ which should give results very close to performing the full linear response with $f_{\rm HX}$, because the interaction is weak and KS levels are well-separated.

Table 3.1: True transition frequencies, KS orbital energy differences, SPA result. $\omega = 1$, $\lambda = 0.1$

True	KS	SPA	Frequency-dependent $f_{\rm XC}$
2.000000	1.975835	1.990861	2.000333
1.981054			1.981388
1.000000	0.980432	1.000342	1.000342

The first excited level is a single excitation, and the SPA gives a very good correction to the ground state KS result. The second set of true levels are mixed single and double excitations, but SPA can only give us one excited level; in this case, it lies in the middle of the two true levels. We shall now explicitly show that it is the lack of frequency-dependence in our approximation to $f_{\rm HXC}$ (Eq. 3.10) that is the culprit.

Consider the slightly more general situation of a Kohn-Sham excited level consisting of a single excitation of frequency ω_q close to a double excitation, and well-separated from all other levels. Let the true excitations near this frequency

be mixtures of the single and double, such that in the non-interacting limit,

$$\begin{aligned} \Psi_a &= m\Phi_D + \sqrt{1-m^2}\Phi_S \\ \Psi_b &= \sqrt{1-m^2}\Phi_D - m\Phi_S, \end{aligned} \tag{3.11}$$

where Φ_S and Φ_D are the wavefunctions of the KS single and double excitations respectively. In our special example above, $m = 1/\sqrt{2}$. We wish to construct the exact exchange-correlation kernel at frequencies near this level. From Eq. 3.1, we have

$$\hat{f}_{\text{HXC}} = \hat{\chi}_{\text{S}}^{-1} - \hat{\chi}^{-1}. \tag{3.12}$$

When the frequency is near ω_q, and this level is well separated from the others, the Lehman sums in χ_{S} and χ are dominated by this level. We may then write

$$\chi_{\text{S}}(x,x';\omega) \approx \frac{A(x,x';\omega)}{\omega-\omega_q}, \tag{3.13}$$

where the matrix $A(x,x';\omega)$ is only very weakly frequency-dependent: $A(x,x';\omega) = \Phi_q(x)\Phi_q(x') + O(\omega-\omega_q)$. Similarly, for the interacting system near this frequency,

$$\chi(x,x';\omega) \approx A(x,x';\omega)\left(\frac{1-m^2}{\omega-\omega_a} + \frac{m^2}{\omega-\omega_b}\right). \tag{3.14}$$

Changing the basis from real space to the space of the KS orbitals, we define a *generalized* SPA (GSPA) as

$$\omega = \omega_q + 2f_{\text{HXC}}(\omega)_{q,q} \tag{3.15}$$

Requiring that the true excitations result if GSPA is used with Eqs.(3.13) and (3.14), determines that $A_{q,q} = 2$ and we will find that f_{HXC} has the form

$$2f_{\text{HXC}}(\omega)_{q,q} = (\bar{\omega}-\omega_q)\left(1 + \frac{\bar{\omega}'\bar{\omega} - \omega_a\omega_b}{(\omega-\bar{\omega}')(\bar{\omega}-\omega_q)}\right). \tag{3.16}$$

where

$$\begin{aligned} \bar{\omega}' &= m^2\omega_a + (1-m^2)\omega_b \\ \bar{\omega} &= (1-m^2)\omega_a + m^2\omega_b, \end{aligned} \tag{3.17}$$

and for the second excited levels, $a = (2, 0), b = (0, 2)$. In the right-hand side of above equations, the first term goes as the interaction strength λ, whereas the second goes as λ^2 which represents the correlation term, and is strongly frequency-dependent. Here we only interested about its behavior, so the actual number is not important to us. In Fig. 3.1, $\chi_{\rm S}^{-1}$ and $f_{\rm HXC}(\omega)$ have been plotted. The two intersections of them (dotted line and solid curve) correspond to the two true transition frequencies. Neglecting the correlation - the λ^2 term in $f_{\rm HXC}$ - then $f_{\rm HXC}$ will become frequency-independent (dashed line), and it has only one intersection with the dotted line $\omega = \bar{\omega}$. That frequency is at the middle of the two true frequencies. This is why we lost the double excitation when we used the adiabatic $f_{\rm HXC}$ in the SPA. If we use the frequency-dependent $f_{\rm HXC}$ in the TDDFT calculation, we can regain the lost double excitation, these results are shown in the last column in Table 3.1, all the calculated transition frequencies are very close to the true values.

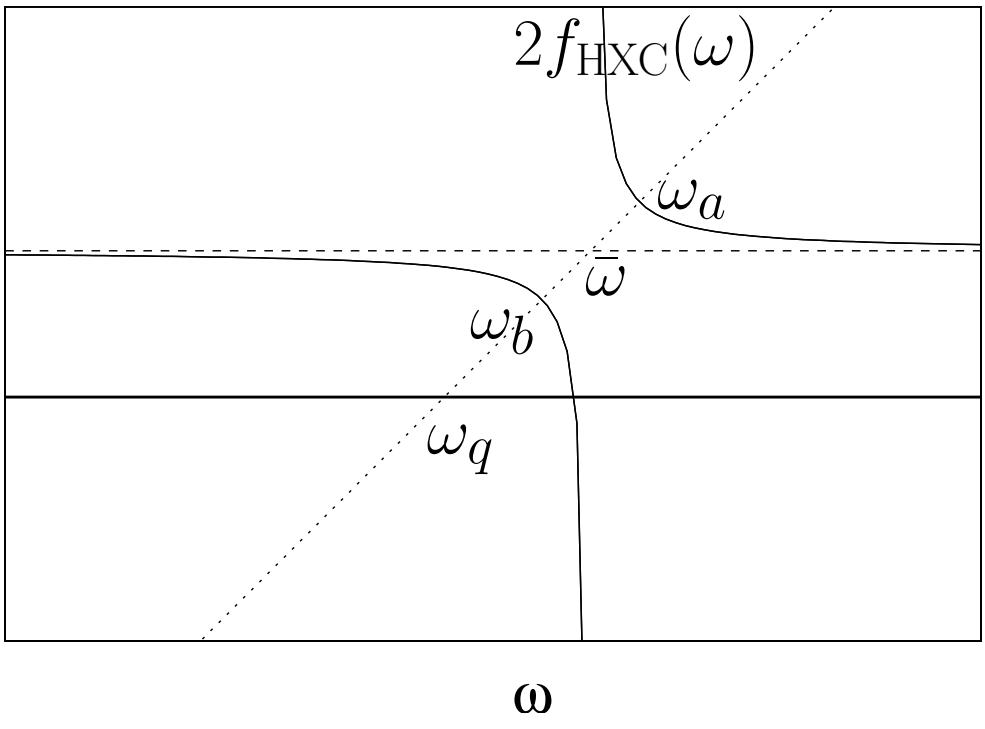

Figure 3.1: How a frequency-dependent $f_{\rm HXC}$ gives us two transition frequencies while the frequency-independent $f_{\rm HXC}$ only gives us one.

This example shows the frequency-dependent behavior that the exact xc kernel must have when a double-excitation is close to a single excitation. We next develop a model for the kernel which uses input from an approximate Kohn-Sham calculation: this yields an approximate xc kernel which is able to produce double excitations. Here we are doing some calculations similar to configuration-interaction (CI). We only use the first 3 HF orbitals, and all the higher excited states has been truncated. So for the two particles, we have the states (0,0), which is the ground state, (0,1), (0,2), which are single excited states, and (1,1), which is the double excited state, and the energy of (1,1) is close to the (0,2) level. Because (0,1) is not coupled with other states, we can just ignore it here. To make it more general, we write the ground state and the single and double excited states as $|0>$, $|q>$ and $|D>$. In the CI calculation, the energies are the eigenvalues of the matrix which are the Hamiltonian in the basis of $|0>$, $|q>$ and $|D>$.

We can rewrite this matrix as

$$\begin{pmatrix} <0|\hat{H}|0> - \frac{<0|\hat{H}|D><D|\hat{H}|0>}{E-<D|\hat{H}|D>} & <0|\hat{H}|q> - \frac{<0|\hat{H}|D><D|\hat{H}|q>}{E-<D|\hat{H}|D>} \\ <q|\hat{H}|0> - \frac{<q|\hat{H}|D><D|\hat{H}|0>}{E-<D|\hat{H}|D>} & <q|\hat{H}|q> - \frac{<q|\hat{H}|D><D|\hat{H}|q>}{E-<D|\hat{H}|D>} \end{pmatrix}. \tag{3.18}$$

This is a two by two matrix, but it has the 3 same eigenvalues as the 3×3 matrix. The main part of the matrix elements only contain single excitations, but the correction part, which is energy-dependent (so also frequency-dependent), contains the double excitation, just like the frequency-dependent part of f_{HXC}. Generally, we can write this part as $\frac{H_{q,D}}{E-H_{D,D}}$, where q is a single excited state and D is a double excited state. By comparison with the SPA formula, we get the frequency-dependent

$$2f_{\text{XC}}(\omega = E - E_0)_{q,q} = 2f_{\text{XC}}^{ASPA}(\omega_q) + \frac{|H_{q,D}|^2}{\omega - (H_{D,D} - H_{0,0})}. \tag{3.19}$$

Now by putting the KS orbitals into eq. (3.19), we get, for $\omega = 1$ and $\lambda = 0.1$, the two transition frequencies from the ground state to the second excited level are 1.98097 and 2.00096, which are very close to the true values in Table 3.1.

The frequency-dependence plays a very important role in the linear response theory in TDDFT. Although the frequency-dependent part is very small (corresponding to the small correlation), it can not be neglect; otherwise, we will lose the information of the multiple excitations. We use a similar method (dressed TDDFT) to treat the double excitation in the system of butadiene and Hexatriene. Compared with the results of TDDFT in Gaussian 98, the dressed TDDFT gives us more accurate energies of the state 2^1A_g [53].

Chapter 4

An Example of Double Excitation: 2^1A_g State of Butadiene

The determination of the character and vertical excitation energy of the low-lying excited states of the short-chain polyenes has posed a considerable challenge to theorists and experimentalists [79, 80, 81, 82, 83]. Hudson and Kohler [81, 82] showed that for octatetraene the lowest singlet excited state was not the HOMO $\rightarrow$ LUMO transition, but was instead a state of the same symmetry as the ground state (1Ag). Configuration Interaction or MCSCF descriptions [79, 80] of this state show considerable contributions of doubly-excited configurations, and indicate that it is purely valence-like.

For the shortest polyenes, butadiene (C_4H_6) and hexatriene (C_6H_8), the position of the 2^1A_g state has been difficult to determine experimentally, although for cis-hexatriene it is known to be the lowest excited singlet state, at least in an adiabatic transition from the ground state [84]. Theoretical estimates of the vertical excitation energy are myriad and varied, but for butadiene recent CI and QDVPT results [85] support the CASPT2 value [86] of approximately 6.3 eV, slightly above the vertical excitation energy of the 1^1B_u (HOMO $\rightarrow$ LUMO) transition (5.92 eV).

Time-Dependent Density Functional Theory (TDDFT) [19, 20] in linear response is an attractive method for the treatment of electronic excitations in molecular systems. However, the adiabatic approximation used in most quantum

chemical calculations (ATDDFT) can not treat states with significant contributions from doubly-excited configurations [88], since the theory is developed in a linear-response formalism to lowest order. In a recent study we have shown that the contributions of higher excitations can be recovered in a linear response formalism if the adiabatic approximation to f_{HXC} is abandoned - i.e. if f_{HXC} is allowed to be frequency/energy dependent. Here we demonstrate that including this frequency dependence in the exchange-correlation kernel yields dramatically improved excitation energies for molecular states possessing significant doubly excited character.

A recent study by Hsu, Hirata, and Head-Gordon [87] applied adiabatic TDDFT to several all-trans polyenes (butadiene to decapentaene). They found reasonable agreement with experiment for the vertical excitation energy to the $2^1\mathrm{A_g}$ state, but only in basis sets containing Rydberg functions, using non-hybrid functionals. The states were largely dominated by one single excitation, in contrast to previous theoretical predictions. Our results show that diffuse functions are not needed to obtain an improved description of the $2^1\mathrm{A_g}$ state, that hybrid functionals can be used, and that the state obtained from our procedure is truly multiconfigurational. In addition, our results show that the theory outlined in [88] represents a practical means of quantitatively correcting adiabatic TDDFT, leading to an improved treatment of higher excitations. We illustrate this using a simple model, outlined below, for butadiene and hexatriene.

To construct the model we performed a series of adiabatic TDDFT calculations to extract energetic parameters and define a model space. Using the PBE015 functional with the 6-311G(d,p) basis (calculations performed using G98 [15]) TDDFT calculations were performed in the truncated space of only two single excitations ($1\mathrm{b_g} \rightarrow 2\mathrm{b_g}$ and $1\mathrm{a_u} \rightarrow 2\mathrm{a_u}$) yielding TDDFT excitation energies to the $2^1\mathrm{A_g}$ state within 0.06 eV of full TDDFT calculations for either butadiene or hexatriene. These two excitations form the model space for our dressed treatment.

Diagonal and off-diagonal TDDFT matrix elements were obtained by fitting to the adiabatic TDDFT energies in this model space. The model reproduced the two-state TDDFT results for the lowest excited $1A_g$ symmetry, and was within 0.1 eV for the second state (since we ignored the modest differences between A and B matrix elements that result from use of a hybrid functional). The equilibrium geometries were taken from experiment [89] for butadiene, and from a B3LYP optimization in the 6-311G(d,p) basis for hexatriene. The TDDFT A and B matrices within this two state model space were then augmented by the dressing proposed in [88], i.e. Xdress was defined as:

$$\begin{bmatrix} \frac{|\langle 1b_g,2b_g|H|D\rangle|^2}{E-E_{\text{double}}} & \frac{\langle 1b_g,2b_g|H|D\rangle\langle D|H|1a_u,2a_u\rangle}{E-E_{\text{double}}} \\ \frac{\langle 1a_u,2a_u|H|D\rangle\langle D|H|1b_g,2b_g\rangle}{E-E_{\text{double}}} & \frac{|\langle 1a_u,2a_u|H|D\rangle|^2}{E-E_{\text{double}}} \end{bmatrix} \tag{4.1}$$

yielding a Dressed TDDFT response matrix of the form:

$$\begin{pmatrix} A+X_{\text{dress}} & B+X_{\text{dress}} \\ B+X_{\text{dress}} & A+X_{\text{dress}} \end{pmatrix}. \tag{4.2}$$

The Hamiltonian matrix elements of the three relevant configurations (two single excitations and one double excitation) were calculated using RHF occupied and virtual orbitals. The double excitation energy in the denominator was estimated as the difference of energy expectation values for the doubly-excited determinant and the ground state RHF determinant, using the RHF orbitals as suggested in [88]. We take the lowest eigenvalue of the dressed TDDFT equations (D-TDDFT) as the energy of the 2^1A_g state. We also dressed the Tamm-Dancoff-TDDFT (TD-TDDFT was introduced by Hirata and Head-Gordon [90]), where only the Dressed TDDFT A matrix is considered (D-TD-TDDFT). Results for the ground state equilibrium geometries for butadiene and hexatriene are given in Table 4.1. For butadiene other methods yield similar results (CASSCF: 6.63 eV, MRSDCI: 6.40 eV [85]) and for hexatriene the experimental vertical excitation energy is 5.21 eV.19 The ATDDFT (PBE0) excitation energies are similar to the

ATDDFT (B3LYP) results (7.22 eV and 6.03 eV for butadiene and hexatriene respectively).

Table 4.1: 2^1A_g state vertical excitation energies (eV) for butadiene and hextriene for all but the CASPT2 results the experimental geometry was used for butadiene (central C-C bond length=1.343A, and C-C bond lengths=1.467A) and a B3LYP/6-311G(d,p) optimized geometry for hexatriene for the present results.

System	CASPT2	ATDDFT(B3LYP)	D-TDDFT	D-TD-TDDFT
C4H6	6.277	7.02	5.93	6.28
C6H8	5.219	5.83	4.85	5.16

The agreement of our D-TDDFT results with previous ab initio results is quite encouraging. Our description yields a state which is a strong mixture of both single and double excitations, which is not dependent upon use of Rydberg basis functions to describe the 2^1A_g state, and is based on PBE0/TDDFT results.

It is known that the 2^1A_g state of butadiene is particularly sensitive to geometry variations [85]. In order to test the ability of D-TDDFT and D-TD-TDDFT to reproduce this geometry dependence, we performed calculations on butadiene analogous to those of Table 4.1, based on an estimate of the planar stationary point for the 21Ag state (central C-C bond length =1.418A, end C-C bond lengths=1.499A, all other lengths and angles are those of the ground state [85]. Results for the vertical excitation energy at this geometry and the 0-0 transition energies are shown in Table 4.2. (The CASPT2 results are based on a slightly different excited state geometry [85]).

Table 4.2: 2^1A_g state vertical and 0-0 excitation energies (eV) for butadiene at the estimated planar stationary point for the 2^1A_g state.

ΔE	CASPT29	ATDDFT(B3LYP)	D-TDDFT	D-TD-TDDFT
Vertical	4.3	5.8	3.42	4.16
0-0	5.2	6.8	4.54	5.28

The MRSDCI estimates (eV) (based on a slightly different excited state geometry) [85] are: Vertical: 4.41 eV, 0-0: 5.21 eV. Clearly the either dressed TDDFT model captures the significant change in 2^1A_g state energy as a function of geometry far better than conventional ATDDFT, with the Tamm-Dancoff version giving somewhat better accuracy in this case.

These results are based on a model calculation, and work is required to implement such a procedure in the context of conventional TDDFT. We next describe the path to be taken in implementing such an approach. First, we are not advocating inclusion of all doubly excited configurations. Inclusion of the entire manifold of double excitations would lead to size-consistency problems similar to those obtained in CISD. Inclusion of only a few important double excitations, those whose transition frequencies lie close to allowed single excitations, while not formally size-consistent, should not cause significant errors since the bulk of the correlation is treated via the XC functional. Second, a complete implementation of such a procedure will utilize matrix elements of KS orbitals for Xdress, rather than the RHF orbitals used here for simplicity. Third, we expect that only a few such double excitations will be important in the description of the low-lying states of conjugated systems. For example, for the treatment of the 1^1B_u state of butadiene (HOMO $\rightarrow$ LUMO) using the Dressed TDDFT model, either of a pair of π double excitations of Bu symmetry lowers the 11Bu state energy by from 0.1-0.3 eV. The ATDDFT (PBE0) 1^1B_u excitation energy in the 6-311G(d,p) basis is 5.98 eV, thus in this case application of the correction would lead to decreased accuracy. However, these double excitations are about 9 eV higher than 1^1B_u state, and further tests of the method may suggest this is outside the range of double excitations that should be included. Furthermore, for Rydberg states the dressing numerators are expected to be small due to the diffuse character of the Rydberg orbitals, and we expect Dressed TDDFT results should reduce to the

TDDFT results. Overall we expect the impact of these terms to be modest except for states of true double excitation character. Nevertheless, for true double excitations we expect that neglection of such terms will lead to states either too high in energy or seriously biased towards Rydberg character.

Thus multiple excitations are included in TDDFT linear response, but only by including frequency-dependent (non-adiabatic) corrections. This correction is derived from first-order Görling-Levy perturbation theory [88], using Kohn-Sham orbitals and energies. Dressing the TDDFT response equations with contributions from low-lying double excitations leads to significant improvement in excitation energies and state characters compared to conventional TDDFT results for the 2^1A_g state of butadiene and hexatriene. Our results suggest that a simple non-empirical correction to linear-response TDDFT allows an accurate treatment of doubly-excited states.

Chapter 5

Adiabatic Connection for Near Degenerate Excited States

Density Functional Theory (DFT) is an efficient and widely used method to calculate the electron structure [2, 3]. By solving the noninteracting system which has the same density as the true system, we can easily get all the ground state properties instead of solve the Schrödinger Equation of the many-electron problem [54]. Although DFT is usually been called ground state DFT, all the excited state properties can also be obtained from the ground state density, since the ground state density determines the external potential, therefore, the Hamiltonian operator [91]. Some routes in DFT to the excited states are ΔSCF, GL PT, variational principle and TDDFT [92, 112, 93, 19]. In our work, we use the 2nd order perturbation theory and the adiabatic connection in DFT to calculate the energies of the near degenerate excited states.

In perturbation theory, we approach the real solution from the Kohn-Sham (KS) system which has the known solutions. The KS equation is

$$\left\{-\frac{1}{2}\nabla^2 + v_{\mathrm{S}}(\mathbf{r})\right\}\phi_i = \epsilon_i\phi_i, \tag{5.1}$$

where the KS potential, $v_{\mathrm{S}} = v_{\mathrm{ext}} + v_{\mathrm{H}} + v_{\mathrm{XC}}$, includes the external, Hartree and exchange-correlation terms. And the ground state density is a summation over the lowest N (N is the number of electrons) KS orbitals,

$$n(\mathbf{r}) = \sum_{i=1}^{N} \phi_i^2(\mathbf{r}). \tag{5.2}$$

The adiabatic connection is a link between the non-interacting KS system and

the fully interacting real system. The Hamiltonian is defined as

$$\hat{H}^{\alpha} = \hat{T} + \alpha \hat{V}_{\rm ee} + \hat{V}^{\alpha}_{\rm ext}, \tag{5.3}$$

where α is the coupling constant and $\hat{V}^{\alpha}_{\rm ext}$ is designed to keep the ground state density independent of α. So at $\alpha = 0$, we have the KS system, while at $\alpha = 1$, we get the real system.

The potential in adiabatic connection can be written as

$$\hat{V}^{\alpha}_{\rm ext} = \hat{V}_{\rm S} - \alpha(\hat{V}_{\rm H} + \hat{V}_{\rm X}) - \hat{V}^{\alpha}_{\rm C}, \tag{5.4}$$

where $\hat{V}^{\alpha}_{\rm C} = \alpha^2 \hat{V}^{(2)}_{\rm C} + \cdots$ includes the 2nd and higher order terms of α [112], and when $\alpha = 1$, $\hat{V}^{\alpha=1}_{\rm C} = \hat{V}_{\rm C}$, the correlation potential. Thus, we have

$$\hat{H}^{\alpha} = \hat{H}_{\rm S} + \alpha(\hat{V}_{\rm ee} - \hat{V}_{\rm HX}) - \hat{V}^{\alpha}_{\rm C}, \tag{5.5}$$

where $\hat{H}_{\rm S} = \hat{T} + \hat{V}_{\rm S} = \hat{H}^{\alpha=0}$ is the Hamiltonian of the KS system.

By using the perturbation theory of nondegenerate states, to the 2nd order of α, we get the energy

$$\begin{aligned} E^{\alpha} &= E_{\rm S} + \alpha \langle \Phi_{\rm S} | \hat{V}_{\rm ee} - \hat{V}_{\rm HX} | \Phi_{\rm S} \rangle - \alpha^2 \langle \Phi_{\rm S} | \hat{V}^{(2)}_{\rm C} | \Phi_{\rm S} \rangle + \\ &\quad + \alpha^2 \sum_{\rm S' \neq S} \frac{|\langle \Phi_{\rm S} | \hat{V}_{\rm ee} - \hat{V}_{\rm HX} | \Phi_{\rm S'} \rangle|^2}{E_{\rm S} - E_{\rm S'}}, \end{aligned} \tag{5.6}$$

where $E_{\rm S}$ and $\Phi_{\rm S}$ are the energy and wavefunction of the KS system.

There are two terms of α^2 in the equation above. In our example, we will show both of them are important and can not be ignored.

For the degenerate (or nearly degenerate) states, the perturbation theory failed if $\langle \Phi_{\rm S} | \hat{V}_{\rm ee} - \hat{V}_{\rm HX} | \Phi_{\rm S'} \rangle$ is nonvanishing while $E_{\rm S}$ and $E_{\rm S'}$ are equal or close. So we diagonalize the perturbation matrix in the subspace of the degenerate states first, and choose the new basis kets that diagonalize the matrix. After that, we apply the formula from the nondegenerate theory, then the contribution from the subspace of the degenerate states will be vanishing automatically in the summation.

We use the 1-dimensinal Hooke's atom as an example to show how our algorithm works. The 1D Hooke's atom contains two electrons, the external potential is a parabolic well, and the repulsion between them is a δ-function. The Hamiltonian is

$$\hat{H} = -\left(\frac{d^2}{dx_1^2} + \frac{d^2}{dx_2^2}\right) + \frac{1}{2}(x_1^2 + x_2^2) + \lambda\delta(x_1 - x_2). \tag{5.7}$$

Transforming to the center of mass and relative coordinates

$$X = (x_1 + x_2)/2, \quad u = x_1 - x_2, \tag{5.8}$$

the Schrödinger Equation can be easily decoupled: the center of mass part is just a harmonic oscillator, and the relative part becomes

$$\left(-\frac{d^2}{du^2} + \frac{1}{4}u^2 + \lambda\delta(u)\right)\phi(u) = E\phi(u). \tag{5.9}$$

The enery eigenvalue of Eq. (5.9) satisfies

$$\lambda = -\frac{2\sqrt{2}\Gamma\left(\frac{3-2E}{4}\right)}{\Gamma\left(\frac{1-2E}{4}\right)}. \tag{5.10}$$

One property of the energy in relative coordinate is for weak λ, the shift from the harmonic oscillator is linear to λ.

So we can solve the 1D Hooke's atom exactly. After calculating the ground state density, we can find the exact KS potential, and all the KS orbitals.

First, we will take a look of the spectrum of the 1D Hooke's atom. To make the problem more simple, we only concentrate on the singlet states. We denote the states of the real system as (N, j), where N and j are the quantum numbers in the center of mass and relative coordinates respectively. The singlet condition means j must be an even number. Now we have the ground state $(0, 0)$, in which both of the center of mass and relative coordinates parts are in their ground states. The only 1st excited state is $(1, 0)$, in which the center of mass coordinate part is on the 1st excited state; and we have 2 excited states for the 2nd excited level, $(2, 0)$ and $(0, 2)$, they have close energies, so we need to use the method of

near degenerate states to treat them. The energy structure of 1D Hooke's atom is shown in Fig. 2.3.

In the KS system, we use another notation for the energy levels. We still use 2 numbers, but they are the KS orbital levels of the 2 electrons. So, $(0,0)$ is also the ground state of the KS system; and the first excited state is $(0,1)$, which means in electron is one the ground state of the KS orbital while the other is in the first excited state; for the 2nd excited state, we have 2 states, one is a single excited state $\Phi_S = (0,2)$, the other is a double excited state $\Phi_D = (1,1)$.

The ground state and first excited state are both nondegenerate, so we can easily apply Eq. (5.6) to them and get the energies up to the second order of α. In practice, it is hard to get $v_{\mathrm{C}}^{(2)}$, so we use an approximation $v_{\mathrm{C}}^{(2)} = v_{\mathrm{C}}$, and in the summation over KS states S', we take the lowest 50 energy levels in the KS system.

The 2nd excited states are near degenerate, so first, we diagonize the perterbation matrix

$$\begin{vmatrix} \langle\Phi_S|H_{\mathrm{S}} + \alpha(V_{\mathrm{ee}} - V_{\mathrm{HX}})|\Phi_S\rangle & \langle\Phi_S|H_{\mathrm{S}} + \alpha(V_{\mathrm{ee}} - V_{\mathrm{HX}})|\Phi_D\rangle \\ \langle\Phi_D|H_{\mathrm{S}} + \alpha(V_{\mathrm{ee}} - V_{\mathrm{HX}})|\Phi_S\rangle & \langle\Phi_D|H_{\mathrm{S}} + \alpha(V_{\mathrm{ee}} - V_{\mathrm{HX}})|\Phi_D\rangle \end{vmatrix}. \tag{5.11}$$

Then the 2 eigenvalues are

$$E_{\pm} = E_c \pm \sqrt{d^2 + \Delta v_{\mathrm{SD}}^2}, \tag{5.12}$$

where

$$E_c = \frac{1}{2}(E_S + \Delta v_{\mathrm{SS}} + E_D + \Delta v_{\mathrm{DD}}), \tag{5.13}$$

$$d = \frac{1}{2}(E_S + \Delta v_{\mathrm{SS}} - E_D - \Delta v_{\mathrm{DD}}), \tag{5.14}$$

$$\Delta v_{\mathrm{SD}} = \alpha\langle\Phi_S|\hat{V}_{\mathrm{ee}} - \hat{V}_{\mathrm{HX}}|\Phi_D\rangle, \tag{5.15}$$

and Δv_{SS} and Δv_{DD} are defined the same way as Δv_{SD}. The new eigenstates are

$$\Phi_+ = \cos\frac{\theta}{2}e^{i\gamma}\Phi_S + \sin\frac{\theta}{2}\Phi_D \tag{5.16}$$

and

$$\Phi_- = -\sin\frac{\theta}{2}e^{i\gamma}\Phi_S + \cos\frac{\theta}{2}\Phi_D \tag{5.17}$$

where

$$\tan\theta = \frac{|\Delta v_{\rm SD}|}{d}, \quad \Delta v_{\rm SD} = |\Delta v_{\rm SD}|e^{-i\gamma}. \tag{5.18}$$

So the perturbated energies are

$$\begin{aligned} E &= E_\pm - \alpha^2\langle\Phi_\pm|\hat{V}_{\rm C}^{(2)}|\Phi_\pm\rangle + \\ &\quad +\alpha^2\sum_{{\rm S}'\neq\pm}\frac{|\langle\Phi_\pm|\hat{V}_{\rm ee}-\hat{V}_{\rm HX}|\Phi_{{\rm S}'}\rangle|^2}{E_\pm - E_{{\rm S}'}} \end{aligned} \tag{5.19}$$

In Table 5.1 and 5.2, we list some approximation results and their errors for the 1D Hooke's atom with $\lambda = 1$ and $\lambda = 0.2$ at $\alpha = 1$ (true system).

Table 5.1: Some approximation results for $\lambda = 1.0$

State	True energy	1st order	error	Include $v_{\rm C}$	error	2nd order	error
(0,0)	1.3067	1.2689	-0.0378	1.3779	0.0712	1.3039	-0.0029
(1,0)	2.3067	2.3055	-0.0013	2.4104	0.1037	2.3064	-0.0003
(0,2)	3.1871	3.1168	-0.0703	3.2056	0.0186	3.2001	0.0130
(2,0)	3.3067	3.3240	0.0173	3.4090	0.1023	3.3047	-0.0020

Table 5.2: Some approximation results for $\lambda = 0.2$

State	True energy	1st order	error	Include $v_{\rm C}$	error	2nd order	error
(0,0)	1.0755	1.0786	0.0031	1.0787	0.0032	1.0758	0.0003
(1,0)	2.0755	2.0800	0.0045	2.0799	0.0044	2.0758	0.0002
(0,2)	3.0395	3.0409	0.0013	3.0399	0.0004	3.0395	-0.0000
(2,0)	3.0755	3.0810	0.0054	3.0800	0.0044	3.0757	0.0001

The column "Include $v_{\rm C}$" is the result which includes the first order term in α and only the $v_{\rm C}$ term from the second order. It does not improve the energy of the first order of α remarkably, and when $\lambda = 1$, some of it's results are even worse then the first order approximation. But if we include the summation term from the second order approximation, we have better result than the first order approximation, (at least 1 more accurate digit).

Fillipi *et al* calculated the excitation energies of the real systems, Helium, ionized lithium and Beryllium, from density functional perturbation theory [94].

They compared two kinds of first-order excitation energies, one is obtained from the standard perturbation theory, (the same way as we get the results of "Include $v_{\rm C}$"), and the other is the first order in the coupling constant, (the same way we get the results of "1st order"). They found the latter is more accurate. Their conclusion coincides with ours.

We plot adiabatic connection of the energies and transition frequencies from the ground state to the second excited states in Fig. 5.1 and 5.2.

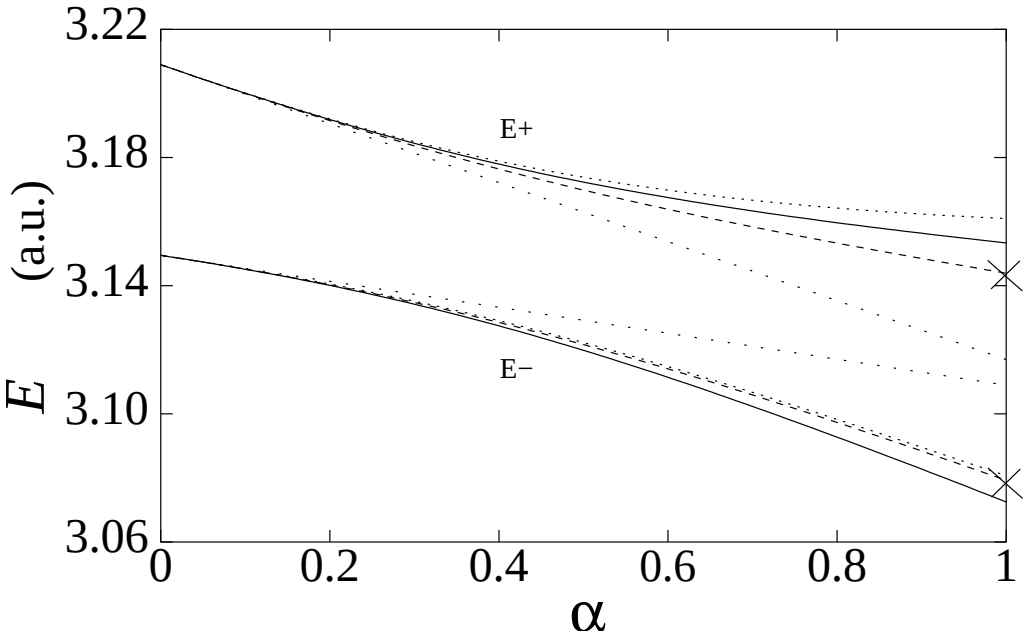

Figure 5.1: The adiabatic connection of the energies when $\lambda = 0.4$ for 2nd excited states

The crosses indicate the true values, the solid lines are $E_{\pm}$, the dashed lines are the results include $v_{\rm C}$ and the dotted lines are got from the 2nd order in α. Compared to the zeroth order approximation ($\alpha = 0$, KS system), the first order approximation has already improved the results a lot. Include $v_{\rm C}$ does not give us a better splitting of the two states. But after adding all the second order terms, we get results which are close to the true values. An important property of the second excitation is the two states are a mixture of the single and double excitations, so if we use some approximation, such as adiabatic single pole approximation, the

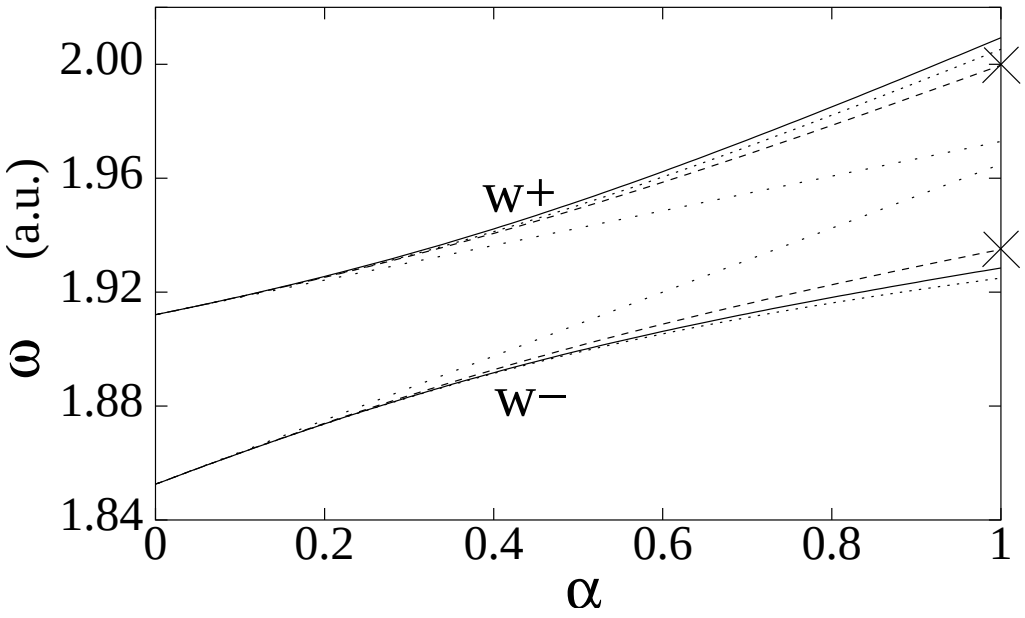

Figure 5.2: The adiabatic connection of the transition frequencies when $\lambda = 0.4$ for 2nd excited states

double excitation will be missing, then we can only get one energy, which is at the middle of the true energies. But the double excitation is not a problem in our calculation, since when we diagonalize the perturbation matrix, we have already mixed the single and double excitations.

The Fig. 5.3 is the energy of the first excited state when $\lambda = 0.4$, which will help us understand that both second order term in α are important. Here, the first order and second order approximations are both close to the true value, but the "Include v_{C}" result has a large error compared to them, this means sometimes the two terms of the second order in α can cancel each other, so when we calculate to the second order in α, we must include both of them.

Our calculation is for the singlet states; for the triplet states, the procedure is the same, the only difference is we need to use another formula when we evaluate $\langle\Phi|\hat{V}_{\mathrm{ee}} - \hat{V}_{\mathrm{HX}}|\Phi\rangle$.

We have shown how to treat nearly degenerate states in Göling-Levy perturbation theory. The calculated results of the simple model show that for some λ,

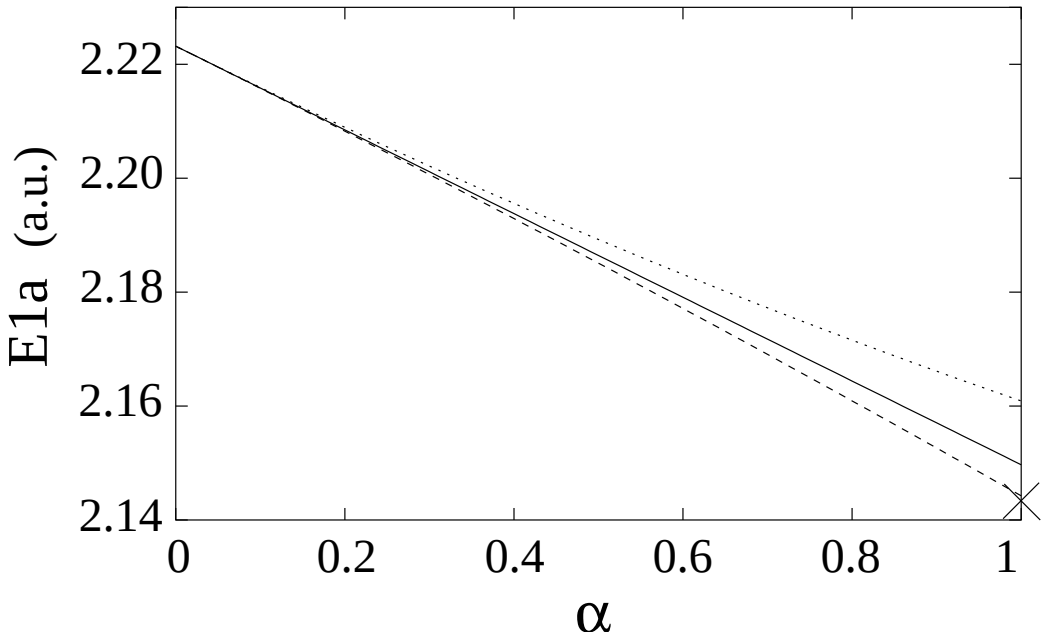

Figure 5.3: The adiabatic connection of the energy when $\lambda = 0.4$ for 1st excited state

which corresponds to the electron repulsion constant, the first order approximation is not accurate enough, we need to use the second order approximation which works well for both nondegenerate and (near) degenerate states. In general, for systems with degeneracies when $\hat{V}_{\text{ee}} = 0$, first-order perturbation theory is inaccurate, even if $\hat{V}_{\text{ee}}$ is very small. The general results can be extended to real atoms and molecules to calculate excitation energies. For example, the methodology applies to stretched H_2 [95], where the ground and first excited states are nearly degenerate.

Chapter 6
TDDFT Calculation of the Scattering Problem

Many works have shown that DFT and TDDFT are very successful in bound-bound transition calculations. In this chapter, we will discuss how to use DFT and TDDFT in the electron-atom scattering problem, where the bound-continuum transitions need to be calculated. The first section is a general introduction to the scattering problems

6.1 General Introduction to Scattering Problem

In scattering problem, what we can count in the experiments is the number dn of particles scattered per unit time into the solid angle $d\Omega$ about the direction (θ, ϕ). dn is obviously proportional to $d\Omega$ and to the incident flux F_i[123],

$$dn = F_i \sigma(\theta, \phi) d\Omega. \tag{6.1}$$

$\sigma(\theta, \phi)$ therefore has the dimensions of a surface, it is called the *differential scattering cross section* in the direction (θ, ϕ). The cross section in the direction $\theta = 0$ (the forward direction) can be obtained by extrapolation from the value of $\sigma(\theta, \phi)$ for small θ.

The *total scattering cross section* σ_{tot} is the sum of cross section over all the directions:

$$\sigma_{\text{tot}} = \int \sigma(\theta, \phi) d\Omega. \tag{6.2}$$

We consider the scattering of a particle of mass m by a potential $V(\mathbf{r})$. Let E be the energy, and $\mathbf{p} = \hbar\mathbf{k}$ the initial momentum of the particle. One can relate

the cross section $\sigma(\Omega)$ to the solution of the Schrödinger equation

$$\left[-\frac{\hbar^2}{2m}\nabla^2 + V(\mathbf{r})\right]\psi_{\mathbf{k}}(\mathbf{r}) = E\psi_{\mathbf{k}}(\mathbf{r}). \tag{6.3}$$

First, we are going to make an assumption that the potential $V(\mathbf{r})$ decreases faster than $1/r$ as $r \to \infty$. Notice that this hypothesis excludes the Coulomb potential. At infinity, the solution of Eq.(6.3) has behavior of the form

$$e^{i\mathbf{k}\cdot\mathbf{r}} + f(\Omega)\frac{e^{ikr}}{r}. \tag{6.4}$$

(In the Coulomb scattering, the Coulomb field has such a long range that it affects the incident and scattered wave even in the asymptotic region, so the solution of Coulomb scattering does not have such behavior. We will treat Coulomb scattering later.)

The two terms of the asymptotic form are easily interpreted if one uses the definition of the current density vector

$$\mathbf{J}(\mathbf{r}) = \frac{\hbar}{2mi}[\psi^*(\mathbf{r})(\nabla\psi(\mathbf{r})) - (\nabla\psi(\mathbf{r}))^*\psi(\mathbf{r})]. \tag{6.5}$$

The plane wave term $\exp(i\mathbf{k}\cdot\mathbf{r})$ represents a wave of unit density and of current density $\hbar\mathbf{k}/m$. Retaining only the lowest order in $1/r$, the term $f(\Omega)\exp(ikr)/r$ represents a wave of density $|f(\Omega)|^2/r^2$ and current density directed along the direction Ω toward increasing r(outgoing wave) and equal to $(\hbar k/m)(|f(\Omega)|^2/r^2)$. Compare the incident and scattered flux, we obtain the scattering cross section

$$\sigma(\Omega) = |f(\Omega)|^2, \tag{6.6}$$

$f(\Omega)$ is called the *scattering amplitude*.

To make the problem simpler, we consider the scattering of a particle by a *central potential* $V(r)$. This asssumption is true for the electron-atom scattering. To calculate the cross section, one needs the asymptotic form of the stationary scattering wave ψ. To this effect we solve the Schrödinger equation in spherical

coordinates. The solution can always be written as

$$\psi(\mathbf{r}) = \sum_{l=0}^{\infty} \sum_{m=-l}^{l} A_{lm} \frac{u_l(r)}{r} Y_l^m(\theta, \phi), \tag{6.7}$$

where u_l satisfies the radial Schrödinger equation

$$\left\{ \frac{\hbar^2}{2m} \frac{d^2}{dr^2} + \left[E - V(r) - \frac{\hbar^2 l(l+1)}{2mr^2} \right] \right\} u_l(r) = 0. \tag{6.8}$$

The solution can also be written in the form (6.7) leaving out all $m \neq 0$ contributions because of the azimuthal symmetry,

$$\psi(\mathbf{r}) = \sum_{l=0}^{\infty} A_l \frac{u_l(r)}{r} P_l(\cos\theta). \tag{6.9}$$

Where we have used the fact that $Y_l^m(\theta, \phi)$ is proportional to $P_l(\cos\theta)$.

Assume the potential vanishes in the region $r > r_{\max}$. Beyond $r_{\max}$, the solution u_l/r can be written as a linear combination of j_l and n_l, the regular and irregular spherical Bessel functions.

$$u_l(r) \propto kr[\cos\delta_l j_l(kr) - \sin\delta_l n_l(kr)]. \tag{6.10}$$

It's asymptotic form

$$u_l(r) \sim \sin(kr - \frac{1}{2} l\pi + \delta_l), \qquad r \to \infty. \tag{6.11}$$

For large r we obtain

$$\begin{aligned}
& \sum_{l=0}^{\infty} A_l \left[\frac{\sin(kr - l\pi/2 + \delta_l)}{kr} \right] P_l(\cos\theta) \\
= \;& e^{i\mathbf{k}\cdot\mathbf{r}} + f(\theta) \frac{e^{ikr}}{r} \\
= \;& \sum_{l=0}^{\infty} (2l+1) i^l j_l(kr) P_l(\cos\theta) + \sum_{l=0}^{\infty} f_l P_l(\cos\theta) \frac{e^{ikr}}{r} \\
= \;& \sum_{l=0}^{\infty} \left[\frac{2l+1}{2ik} (-)^{l+1} e^{-ikr} + \left(f_l + \frac{2l+1}{2ik} \right) e^{ikr} \right] \times \\
& P_l(\cos\theta).
\end{aligned} \tag{6.12}$$

For each l, ,the left-hand and right-hand sides must equal, so we have

$$A_l = (2l+1) e^{i\delta_l} i^l, \tag{6.13}$$

and

$$f_l = \frac{2l+1}{k} e^{i\delta_l} \sin\delta_l. \tag{6.14}$$

The differential cross section is obtained by forming the square modulus of $f(\theta)$,

$$\sigma(\Omega) = \frac{1}{k^2} \left| \sum_{l=0}^{\infty} (2l+1) e^{i\delta_l} \sin\delta_l P_l(\cos\theta) \right|^2. \tag{6.15}$$

Integration over the angles (θ, ϕ) yields the total cross section $\sigma_{\rm tot}$. Using the orthonormality relations of the Legendre polynomials, we find

$$\sigma_{\rm tot} = \frac{4\pi}{k^2} \sum_{l=0}^{\infty} (2l+1) \sin^2\delta_l. \tag{6.16}$$

In most of the problems, the s-wave phase shift (δ_0) plays the most important role, so in this section, we use it to check how DFT works in scattering problem.

Now back to the coulomb scattering problems. After reduction to the center of mass, the Schrödinger equation of the collision of two particles with Coulomb interaction can be written as

$$\left[-\frac{\hbar^2}{2m}\Delta + \frac{Z_1 Z_2 e^2}{r} \right] \psi(\mathbf{r}) = E\psi(\mathbf{r}), \tag{6.17}$$

where E is the energy in the center of mass system. The scattering cross section is related to the asymptotic behavior of the eigensolutions of positive energy. Let us take

$$E = \frac{\hbar^2 k^2}{2m} = \frac{1}{2} m v^2, \tag{6.18}$$

$$\gamma = \frac{Z_1 Z_2 e^2}{\hbar v}, \tag{6.19}$$

It can be proved that the Coulomb scattering amplitude

$$f_{\rm c}(\theta) = -\frac{\gamma}{2k \sin^2\frac{\theta}{2}} \exp[-i\gamma \ln(\sin^2\frac{\theta}{2}) + 2i\sigma_0], \tag{6.20}$$

where

$$\sigma_0 = \arg\Gamma(1+i\gamma). \tag{6.21}$$

Thus the Coulomb scattering cross section:

$$\begin{aligned}\sigma_{\rm c}(\Omega) &= |f_{\rm c}(\theta)|^2 \\ &= \frac{\gamma^2}{4k^2\sin^4\frac{\theta}{2}} \\ &= \left(\frac{Z_1Z_2e^2}{4E}\right)^2 \frac{1}{\sin^4\frac{\theta}{2}}. \end{aligned} \tag{6.22}$$

This turns out to be identical to the Rutherford formula of classical Coulomb scattering cross section.

When a short-range interaction $V'(r)$ is added to the Coulomb field $V_{\rm c}(r)$, we have

$$f(\theta) = f_{\rm c}(\theta) + f'(\theta), \tag{6.23}$$

$$f'(\theta) = \frac{1}{2ik}\sum_{l=0}^{\infty}(2l+1)e^{2i\sigma_l}(e^{2i\delta_l}-1)P_l(\cos\theta), \tag{6.24}$$

where $\sigma_l = \arg\Gamma(l+1+i\gamma)$ is the *Coulomb phase shift*, and δ_l is the phase shift from Coulomb scattering. The scattering cross section is

$$\sigma(\Omega) = |f(\theta)|^2 \tag{6.25}$$

$$= \sigma_{\rm c}(\Omega) + 2\Re f_{\rm c}^* f' + |f'(\theta)|^2. \tag{6.26}$$

So for both short-ranged and Coulomb scattering problem, all we need to calculate is the phase shifts δ_l, but they have different meanings in these two kinds of problems. For short-ranged scattering, it is the phase shift from the Bessel function, but in Coulomb scattering, it is the phase shift from the Coulomb wave function.

6.2 TDDFT Calculation

For the electron-atom scattering problem, we choose the electron and atom together as our system. So the KS system also contains $N+1$ electrons, and the electron is scattered by the KS potential of the $N+1$ system. (Here we assume

the ground state of the $N+1$ electron system is also bound, so its ground state electronic density exist.) After we get the phase shift of the KS system, we will use TDDFT linear response to add the exchange-correlation corrections to it and to obtain the phase shift of the real scattering problem.

The susceptibility $\chi_{\rm S}$ of the KS system can be expressed by the Green function:

$$\chi_{\rm S}(\mathbf{r},\mathbf{r}';\omega) = 2\sum_{iocc}\phi^*_{si}(\mathbf{r})\phi_{si}(\mathbf{r}')g_{\rm S}(\mathbf{r},\mathbf{r}';\epsilon_i+\omega) + c.c(\omega\to-\omega). \tag{6.27}$$

In the electorn-atom scattering, the KS system s spherically symmetric, so the Green function can be expanded in spherical harmonics as

$$g_{\rm S}(\mathbf{r},\mathbf{r}';\omega) = \sum_{l=0}^{\infty}\sum_{m=-l}^{l} g_{sl}\mathcal{Y}^{\hat{\mathbf{r}}\hat{\mathbf{r}}'}_{lm}, \tag{6.28}$$

with $\mathcal{Y}^{\hat{\mathbf{r}}\hat{\mathbf{r}}'}_{lm} \equiv Y^m_l(\hat{\mathbf{r}})Y^{m*}_l(\hat{\mathbf{r}}')$.

When the magnitude of $\mathbf{r}$ is very large, $g^*(-\omega)$ will become exponentially small and the dominate term in $\chi_{\rm S}$ is the KS HOMO orbital, so we have

$$\chi_{\rm S}(\mathbf{r},\mathbf{r}';\omega) \underset{r\to\infty}{\to} \frac{\sqrt{\rho(r)}u_{sH}(r')}{rr'}\mathcal{Y}^{*\hat{\mathbf{r}}\hat{\mathbf{r}}'}_{l_Hm_H}\sum_{lm} g_{sl}(r,r';\omega-I)\mathcal{Y}^{\hat{\mathbf{r}}\hat{\mathbf{r}}'}_{lm}. \tag{6.29}$$

Where I is the first ionization energy of the $N+1$ electron system, and $u_{sH}(r)$ is the radial KS HOMO orbital, $\phi_{sH}(\mathbf{r}) = r^{-1}u_{sH}Y^{m_H}_{l_H}(\hat{\mathbf{r}})$. Also, when both of r and r' are large, we have

$$\chi_{\rm S}(\mathbf{r},\mathbf{r}';\omega) \underset{r,r'\to\infty}{\to} \frac{\sqrt{\rho(r)\rho(r')}}{rr'}\mathcal{Y}^{*\hat{\mathbf{r}}\hat{\mathbf{r}}'}_{l_Hm_H}\sum_{lm} g_{sl}(r,r';\omega-I)\mathcal{Y}^{\hat{\mathbf{r}}\hat{\mathbf{r}}'}_{lm}. \tag{6.30}$$

We make an assumption here that the susceptibility χ of the real scattering system also has similar behavior at large distance r as the KS susceptibility $\chi_{\rm S}$, i.e.

$$\chi(\mathbf{r},\mathbf{r}';\omega) \underset{r\to\infty}{\to} \frac{\sqrt{\rho(r)}u_{H}(r')}{rr'}\mathcal{Y}^{*\hat{\mathbf{r}}\hat{\mathbf{r}}'}_{l_Hm_H}\sum_{lm} g_{l}(r,r';\omega-I)\mathcal{Y}^{\hat{\mathbf{r}}\hat{\mathbf{r}}'}_{lm}. \tag{6.31}$$

and

$$\chi(\mathbf{r},\mathbf{r}';\omega) \underset{r,r'\to\infty}{\to} \frac{\sqrt{\rho(r)\rho(r')}}{rr'}\mathcal{Y}^{*\hat{\mathbf{r}}\hat{\mathbf{r}}'}_{l_Hm_H}\sum_{lm} g_{l}(r,r';\omega-I)\mathcal{Y}^{\hat{\mathbf{r}}\hat{\mathbf{r}}'}_{lm}. \tag{6.32}$$

In TDDFT linear response, χ and $\chi_{\rm S}$ are related through a Dyson-like equation

$$\chi(\mathbf{r},\mathbf{r}';\omega)=\chi_{\rm S}(\mathbf{r},\mathbf{r}';\omega)+\int d^3r_1\int d^3r_2\chi_{\rm S}(\mathbf{r},\mathbf{r}_1;\omega)f_{\rm HXC}(\mathbf{r}_1,\mathbf{r}_2;\omega)\chi(\mathbf{r}_2,\mathbf{r}';\omega). \tag{6.33}$$

Take the limit of $r,r'\to\infty$, put Eqs. (6.29)-(6.32) into it and compare the coefficient of the solid angle $d\Omega$, we can have

$$\begin{aligned}\lim_{r,r'\to\infty}g_l(r,r';\epsilon) &= \lim_{r,r'\to\infty}g_{sl}(r,r';\epsilon)+\lim_{r,r'\to\infty}\int d^3\mathbf{r}_1\int d^3\mathbf{r}_2\frac{u_{sH}(r_1)u_H(r_2)}{r_1r_2}\\ &\times g_{sl}(r,r_1;\epsilon)f_{\rm HXC}(\mathbf{r}_1,\mathbf{r}_2;\epsilon+I)g_l(r_2,r';\epsilon)\mathcal{Y}^{\hat{\mathbf{r}}_1\hat{\mathbf{r}}_2}_{l_Hm_H}\mathcal{Y}^{*\hat{\mathbf{r}}_1\hat{\mathbf{r}}_2}_{l0},\end{aligned} \tag{6.34}$$

where $\epsilon=\omega-I$ is the energy of the scattered electron.

The radial KS Green function $g_{sl}(r,r';\epsilon)$ can be written as [126, 125]

$$g_{sl}(r,r';\epsilon)=-2(rr'W_s)^{-1}u^{(1)}_{skl}(r_<)u^{(2)}_{skl}(r_>), \tag{6.35}$$

where $u^{(1)}_{skl}$ and $u^{(2)}_{skl}$ are regular and irregular solutions of the radial Schrödinger equation with the ground state $N+1$ electron KS potential $v_{\rm S}(r)$ respectively. And their asymptotic behaviors at large r are

$$u^{(1)}_{skl}(r)\underset{r\to\infty}{\to}k^{-1}e^{i\delta_{sl}}\sin(h_{kl}(r)+\delta_{sl}) \tag{6.36}$$

and

$$u^{(2)}_{skl}(r)\underset{r\to\infty}{\to}k^{-1}e^{i(h_{kl}(r)+2\delta_{sl})}, \tag{6.37}$$

with

$$h_{kl}(r)=kr-\frac{l\pi}{2}+\gamma\left(\frac{\ln 2kr}{k}+\sigma_l\right), \tag{6.38}$$

where γ depends on whether the KS potential of the $N+1$ electron system is short-ranged ($\gamma=0$) or with a Coulomb tail ($\gamma=1$), and δ_{sl} is the KS phase shift. In Eq. (6.35), $W_s=k^{-1}\exp(2i\delta_{sl})$ is the Wronskian between $u^{(1)}_{skl}$ and $u^{(2)}_{skl}$.

Assume $r>r'$, we have the asymptotic behavior of Green functions

$$g_{sl}(r,r';\epsilon)\underset{r\to\infty}{\to}-2(rr')^{-1}e^{ih_{kl}(r)}u^{(1)}_{skl}(r'), \tag{6.39}$$

$$g_{sl}(r,r';\epsilon)\underset{r>r'\to\infty}{\to}-2(krr')^{-1}e^{i(h_{kl}(r)+\delta_{sl})}\sin(h_{kl}(r')+\delta_{kl}), \tag{6.40}$$

$$g_l(r,r';\epsilon) \underset{r\to\infty}{\to} -2(rr')^{-1}e^{ih_{kl}(r)}u_{kl}^{(1)}(r'), \tag{6.41}$$

$$g_l(r,r';\epsilon) \underset{r>r'\to\infty}{\to} -2(krr')^{-1}\ e^{i(h_{kl}(r)+\delta_l)}\sin(h_{kl}(r')+\delta_l). \tag{6.42}$$

Inserting Eqs. (6.39)-(6.42) to Eq. (6.34) yields

$$e^{i\delta_l}\sin(h_{kl}(r)+\delta_l) = e^{i\delta_{sl}}\sin(h_{kl}(r)+\delta_{sl}) - 2ke^{ih_{kl}(r)}\langle\langle f_{\text{HXC}}\rangle\rangle_l, \tag{6.43}$$

where

$$\langle\langle f_{\text{HXC}}\rangle\rangle_l \equiv \int d^3r_1 \int d^3r_2 \frac{u_{sH}(r_1)u_H(r_2)}{(r_1r_2)^2} u_{skl}^{(1)}(r_1) f_{\text{HXC}}(\mathbf{r}_1,\mathbf{r}_2;\epsilon+I) u_{kl}^{(1)}(r_2) \mathcal{Y}_{l_H m_H}^{\hat{\mathbf{r}}_1\hat{\mathbf{r}}_2} \mathcal{Y}_{l0}^{*\hat{\mathbf{r}}_1\hat{\mathbf{r}}_2} \tag{6.44}$$

In the formula of $\langle\langle f_{\text{HXC}}\rangle\rangle_l$, u_H and $u_{kl}^{(1)}$ are orbital and scattering wave function of the real system, we then approximate of the functions in KS system:

$$u_H(r) \sim u_{sH}(r), \qquad u_{kl}^{(1)} \sim u_{skl}^{(1)}(r). \tag{6.45}$$

And we define energy normalized wave function

$$\tilde{u}_{skl}^{(1)} = \sqrt{\frac{2k}{\pi}} e^{i\delta_{sl}} u_{skl}^{(1)}(r) \underset{r\to\infty}{\to} \sqrt{\frac{2}{\pi k}} \sin(h_{kl}(r)+\delta_{sl}). \tag{6.46}$$

and

$$[[f_{\text{HXC}}]]_l \equiv \frac{2k}{\pi} e^{-i(\delta_l+\delta_{sl})} \langle\langle f_{\text{HXC}}\rangle\rangle_l, \tag{6.47}$$

then all the r-dependent terms in Eq. (6.43) will be canceled, so we can simplify Eq. (6.43) to

$$\sin(\delta_{sl}-\delta_l) = 2\pi[[f_{\text{HXC}}]]_l. \tag{6.48}$$

This equation tells us how to add in TDDFT correction to KS phase shift to calculate the phase shift of the real scattering problem.

6.3 Results

We do calculations on e-He+ and e-H scatterings to show how our TDDFT method works. The ground state KS system is then the Helium and H+, and

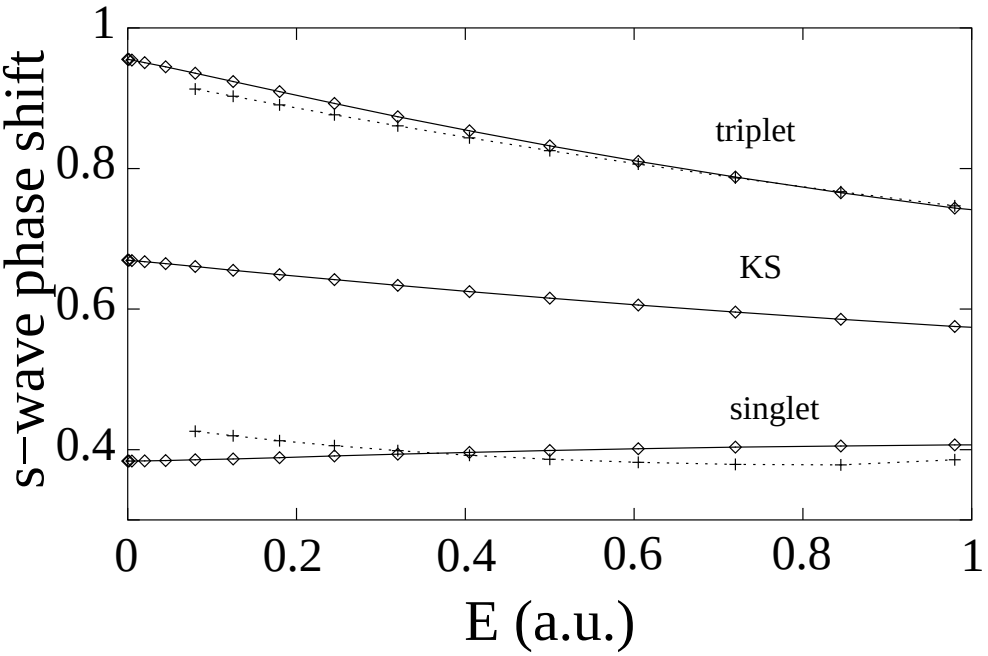

Figure 6.1: The s-wave phase shift of e-H scattering

we use the exact KS potentials. When calculate the kernel, we use hybrid functional as the exchange-correlation kernel [101].

In Fig. 6.1, the s-wave phase shifts of e-He+ scattering have been plotted, the dotted lines are from [100], and the solid lines are DFT and TDDFT phase shifts. Just as bound-bound transitions, the KS phase shifts lies between the exact singlet and triplet phase shift. After we applied the TDDFT corrections to it,we get very good results for both singlet and triplet phase shifts. One thing we must notice here is e-He+ is a Coulomb scattering problem, and the exact KS potential of He has a Coulomb tail, but if we use LDA or GGA approximation, the KS potential will decay exponentially when r goes large, so the KS phase shift will become short-ranged and can not be compared to the real phase shift (which is from Coulomb scattering). So If we use LDA or GGA KS potential for the Coulomb scattering problem, we need add a Coulomb tail to the KS potential so that it will have asymptotically correct behavior at large r.

We also compute the e-H phase shifts. In Fig. 6.2, the dotted lines are from

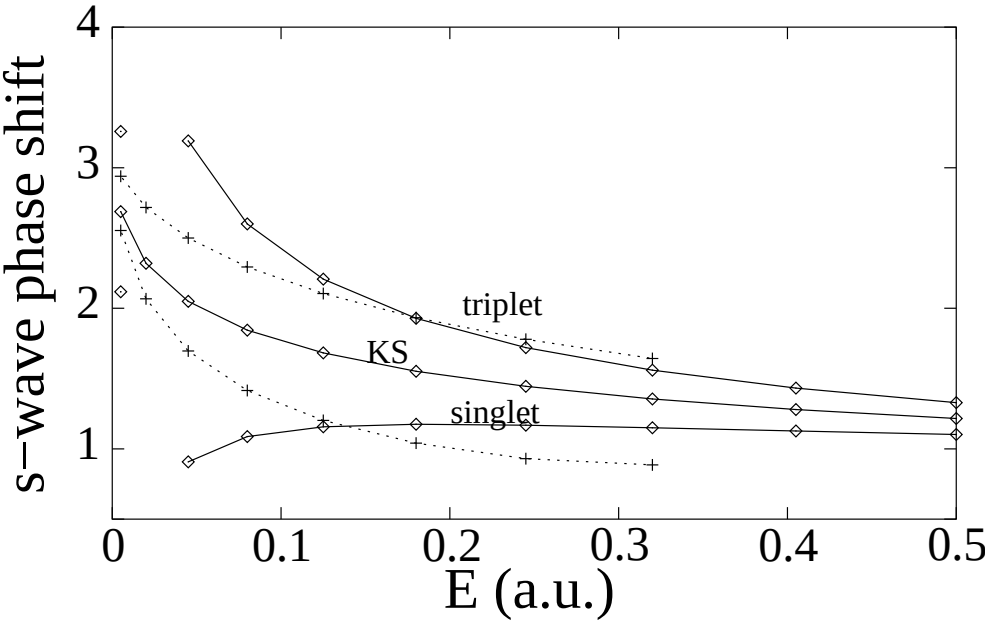

Figure 6.2: The s-wave phase shift of e-He+ scattering

[99], and solid lines are DFT and TDDFT results. The KS phase shift from DFT are still good, but the TDDFT does not give good corrections. We also plot the $[[f_{\text{HXC}}]]_0$ terms in Fig. 6.3, we can see that it has a peak at low energy, and near that peak, $2\pi[[f_{\text{HXC}}]]$ is larger than 1, so the TDDFT fomula Eq. (6.43) fails. Also, when energy goes large, $[[f_{\text{HXC}}]]_0$ decrease too fast. We tried differnt exchange-correlation kernels, (such as ALDA and exact exchange), both of them have similar errors as the hybrid functional, so these errors may come from that Eq. (6.45) is not a good approximation for the e-H approximation.

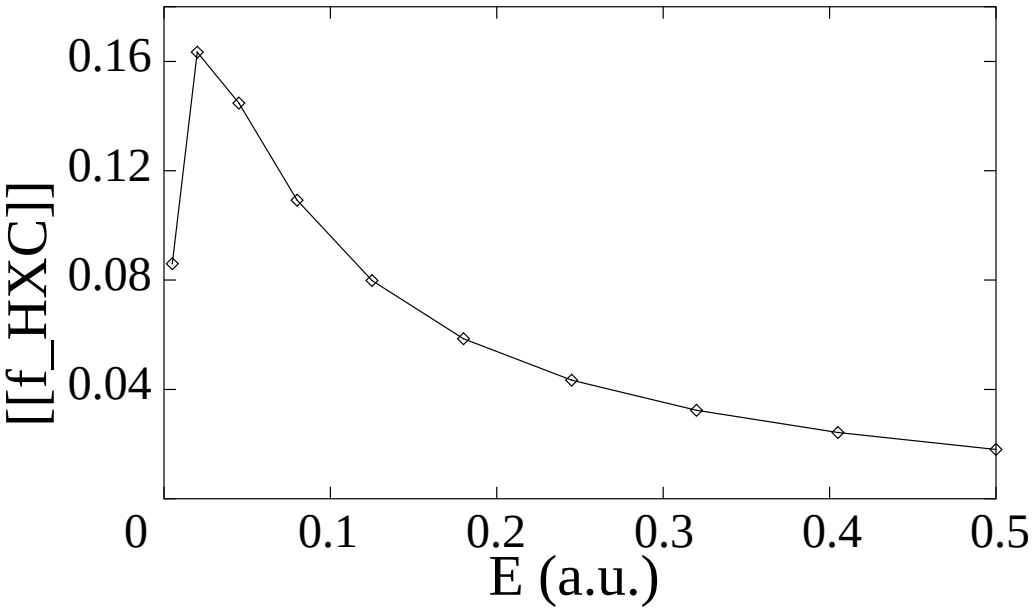

Figure 6.3: $[[f_{\mathrm{HXC}}]]$ of e-H scattering

Appendix A
Code for Scattering Calculation

We make a program in Fortran to calculate the phase shift in scattering problem. Here are some details about the code.

A.1 Numerical Methods

A.1.1 Numerov's Algorithm for the Radial Schrödinger Equation [124]

The radial Schrödinger equation

$$\left\{\frac{\hbar^2}{2m}\frac{d^2}{dr^2}+\left[E-V(r)-\frac{\hbar^2 l(l+1)}{2mr^2}\right]\right\}u_l(r)=0. \tag{A.1}$$

can be solved numerically by Numerov's method. This is an efficient method for solving equations of the type

$$\ddot{x}(t)=f(t)x(t). \tag{A.2}$$

Numerov's method makes use of the special structure of this equation in order to have the fourth order contribution to $x(h)$ cancel, leading to a form similar to the Verlet algorithm, but accurate to order h^6 (only even orders of h occur because of time-reversal symmetry). The Verlet algorithm was derived by expanding $x(t)$ up to second order around $t=0$ and adding the resulting expression for $t=h$ and $t=-h$. If we do the same for Eq. (A.2) but now expand $x(t)$ to order six in t, we obtain

$$x(h)+x(-h)-2x(0)$$

$$= \quad h^2 f(0)x(0) + \frac{h^4}{12}x^{(4)}(0) + \frac{h^6}{360}x^{(6)}(0) + O(h^8) \tag{A.3}$$

with $x^{(4)}$ being the fourth and $x^{(6)}$ the sixth derivative of x with respect to t. As these derivatives are not known, this formula is not useful as such. However, after switching to another variable $w(t) = [1 - h^2 f(t)/12]x(t)$, Eq. (A.3) becomes

$$w(h) + w(-h) - 2w(0) = h^2 f(0)x(0) + O(h^6), \tag{A.4}$$

so that, using a second order integration scheme for w (i.e. using only two values of the solution to predict the next one), $x(h)$ is known to order h^6. Whenever $x(t)$ is required, it can be calculated as $x(t) = w(t)/[1 - h^2 f(t)/12]$.

A.1.2 Calculate Phase Shift

It can be proved that in the radial Schrödinger Eq. (A.1), if

$$\lim_{r\to 0} r^2 V(r) = 0, \tag{A.5}$$

then the solution $u_l(r)$ satisfies

$$\lim_{r\to 0} u_l(r) \sim r^{l+1}. \tag{A.6}$$

so we can always choose the initial value of the wave function as $u_l(0) = 0$, $u_l(h) = h^{l+1}$. After we solve the differential equation numerically, the wave function may not be normalized. To determine the phase shift, we choose two point $r_1,\ r_2 > r_{\max}$, (the short range potential vanishes beyond $r_{\max}$,) then

$$\begin{aligned} u_l(r_1) &= A\cos\delta_l F_R(r_1) + A\sin\delta_l F_I(r_1), \\ u_l(r_2) &= A\cos\delta_l F_R(r_2) + A\sin\delta_l F_I(r_2). \end{aligned} \tag{A.7}$$

Where $F_R(r) = r j_l(r),\ F_I(r) = -r n_l(r)$ for non-Coulomb scattering and $F_R(r) = F_l(r),\ F_I(r) = G_l(r)$ for coulomb scattering. So we have

$$\begin{aligned} A\sin\delta_l &= \frac{u_l(r_1)F_R(r_2) - u_l(r_2)F_R(r_1)}{F_I(r_1)F_R(r_2) - F_I(r_2)F_R(r_1)}, \\ A\cos\delta_l &= \frac{u_l(r_2)F_I(r_1) - u_l(r_1)F_I(r_2)}{F_I(r_1)F_R(r_2) - F_I(r_2)F_R(r_1)}, \end{aligned} \tag{A.8}$$

$$\tan\delta_l = \frac{u_l(r_1)F_R(r_2) - u_l(r_2)F_R(r_1)}{u_l(r_2)F_I(r_1) - u_l(r_1)F_I(r_2)}. \tag{A.9}$$

And because $F_I(r_1)F_R(r_2) - F_I(r_2)F_R(r_1) \sim \sin(k(r_2 - r_1))$, so we should choose $r_2 - r_1 \sim \pi/2k$.

A.2 Special Functions

Here are some special functions we need in the scattering calculation.

A.2.1 Spherical Bessel Functions

The solutions of differential equation

$$x^2w'' + 2xw' + [x^2 - l(l+1)]w = 0 \tag{A.10}$$

are the Spherical Bessel functions of the first kind

$$j_l(x) = \sqrt{\frac{\pi}{2x}}J_{l+\frac{1}{2}}(x) \tag{A.11}$$

and the Spherical Bessel functions of the second kind

$$n_l(x) = \sqrt{\frac{\pi}{2x}}Y_{l+\frac{1}{2}}(x). \tag{A.12}$$

Rayleigh's formulas

$$\begin{aligned} j_l(x) &= x^l\left(-\frac{1}{x}\frac{d}{dx}\right)^l\frac{\sin x}{x}, \\ n_l(x) &= -x^l\left(-\frac{1}{x}\frac{d}{dx}\right)^l\frac{\cos x}{x}, \quad (l = 0, 1, 2, \ldots). \end{aligned} \tag{A.13}$$

The first several Spherical Bessel functions are

$$\begin{aligned} j_0(x) &= \frac{\sin x}{x}, \\ j_1(x) &= \frac{\sin x}{x^2} - \frac{\cos x}{x}, \\ j_2(x) &= \left(\frac{3}{x^3} - \frac{1}{x}\right)\sin x - \frac{3}{x^2}\cos x, \end{aligned}$$

$$
\begin{aligned}
n_0(x) &= -\frac{\cos x}{x}, \\
n_1(x) &= -\frac{\cos x}{x^2} - \frac{\sin x}{x}, \\
j_2(x) &= \left(-\frac{3}{x^3} + \frac{1}{x}\right)\cos x - \frac{3}{x^2}\sin x.
\end{aligned} \tag{A.14}
$$

The recurrence relations

$$
f_{l-1}(x) + f_{l+1}(x) = (2l+1)x^{-1} f_l(x), \quad (l = 0, \pm 1, \pm 2, \ldots) \tag{A.15}
$$

where $f_l(x)$ stands for $j_l(x)$ and $n_l(x)$.

A.2.2 Coulomb Wave Functions

The differential equation is

$$
\frac{d^2 w}{d\rho^2} + [1 - \frac{2\eta}{\rho} - \frac{l(l+1)}{\rho^2}]w = 0. \tag{A.16}
$$

The general solution is

$$
w = C_1 F_l(\eta, \rho) + C_2 G_l(\eta, \rho), \quad (C_1, C_2 \text{ constants}) \tag{A.17}
$$

where $F_l(\eta, \rho)$ is the regular Coulomb wave function and $G_l(\eta, \rho)$ is the irregular Coulomb wave function.

So for the problem that an electron is scattered by a coulomb potential $-Z/r$, the radial Schrödinger equation is

$$
\left[\frac{1}{2}\frac{d^2}{dr^2} + \left(E + \frac{Z}{r} - \frac{l(l+1)}{2r^2}\right)\right] u_l(r) = 0, \tag{A.18}
$$

and the solutions are $F_l(-\frac{Z}{\sqrt{2E}}, \sqrt{2E}r)$ and $G_l(-\frac{Z}{\sqrt{2E}}, \sqrt{2E}r)$.

We use *GNU scientific library* (gsl) [102] calculate the special functions values in our code.

A.3 Code Testing

A.3.1 Short Range Potential

We use Hard sphere to check the error of the code, since the analytic solution is known.

(1) $a = 1$, $L = 0$, $dx = .5,\ .2,\ .1$

Found $\Delta\delta_{L=0}$ grows with E depending on dx.

Define E_c = energy at which $\sim 10\%$ error in δ.

For $dx = .5$, $E_c \sim 5$; $dx = .2$, $E_c \sim 20$; $dx = .1$, $E_c \sim 80$. So $E_c \sim (dx)^{-2}$, error $\propto kdx$.

(2) Repeat (1) for $L_{\max} = 5$, no dependence on L.

(3) Take $L_{\max} = 5$, $\Delta\sigma/\sigma = 1\%$ at $E = 42.8$ for $dx = .125$; at $E = 6.7$ for $dx = .25$; at $E = 1.4$ for $dx = .5$. Better than $(dx)^{-2}$.

Table A.1: Error of total cross section for the hard sphere scattering when $a = 1.0$, $L = 5$.

E	Δx=0.05	0.1	0.2	0.4	0.8	1.6
1	-0.00000	-0.00008	-0.0012	-0.018	-0.19	+
2	-0.000014	-0.00022	-0.0035	-0.054	-0.62	+
3	-0.000030	-0.00047	-0.0077	-0.14	-1.63	+
4	-0.000050	-0.00082	-0.013	-0.20	-0.90	+

In Table A.1, the errors of the total cross section for different energy and dx are listed. We found $\Delta\sigma_{\text{tot}} \propto (dx)^4$ and $\Delta\sigma_{\text{tot}} \propto E^{1.7}$.

A.3.2 Coulomb Potential

In Table A.2, the errors of the phase shift are listed. Since this is pure Coulomb scattering, so the analytic solution is $\delta_l = 0$. We found

(1) when $0.001 \leq dx \leq 0.08$, $\Delta\delta_l \propto (dx)^4$ and $\Delta\delta_l \propto E^{2.4}$.

(2) For same E and dx, $\Delta\delta_l$ decrease when l increase, but the change is small.

Usually, increasing $x_{\max}$ will increase the error. This comes from the error of solving the differential equation. $\Delta\delta_l \sim 2 \times 10^{-11}$ when $E = 1$, $dx = 0.001$, $l = 1, \ldots, 5$ and $x_{\max} = 2000$, so $\Delta\delta_l$ increase linear to $x_{\max}$. $x_{\max} = 20$ should be enough for most of the problems.

Table A.2: Error of phase shift for the electron-H+ scattering when $x_{\max} = 20$.

E	L	Δx=0.001	0.01	0.02	0.04	0.08	0.16
1	0	3.01e-13	3.07446e-09	4.92049e-08	7.88818e-07	1.26765e-05	-0.02260564
	1	3.25157e-13	3.24674e-09	5.20299e-08	8.34144e-07	1.34005e-05	0.001439116
	2	2.70057e-13	2.69981e-09	4.31788e-08	6.90521e-07	1.10401e-05	0.000176574
	3	2.21661e-13	2.22937e-09	3.57466e-08	5.73697e-07	9.23753e-06	0.000149799
	4	1.97268e-13	1.96197e-09	3.13804e-08	5.01788e-07	8.01995e-06	0.000128123
	5	1.65117e-13	1.65919e-09	2.66189e-08	4.27535e-07	6.8946e-06	0.00011214
2	0	1.6328e-12	1.63667e-08	2.61792e-07	4.19781e-06	6.72064e-05	-0.02240787
	1	1.54713e-12	1.55035e-08	2.48109e-07	3.96901e-06	6.35772e-05	0.003131033
	2	1.39959e-12	1.40255e-08	2.24533e-07	3.60706e-06	5.80232e-05	0.00093888
	3	1.23061e-12	1.23211e-08	1.97132e-07	3.15141e-06	5.04113e-05	0.000808317
	4	1.12413e-12	1.12747e-08	1.80533e-07	2.90294e-06	4.67622e-05	0.000758797
	5	1.01313e-12	1.01477e-08	1.62355e-07	2.59498e-06	4.1501e-05	0.000665188
3	0	4.22094e-12	4.24104e-08	6.79238e-07	1.08907e-05	0.000175064	-0.02142527
	1	4.13548e-12	4.13829e-08	6.62088e-07	1.05932e-05	0.000169551	0.005784012
	2	3.66698e-12	3.67535e-08	5.88692e-07	9.44173e-06	0.000151935	0.002467564
	3	3.4554e-12	3.45807e-08	5.53408e-07	8.85858e-06	0.000141893	0.002277795
	4	3.08719e-12	3.09485e-08	4.95717e-07	7.95088e-06	0.000127968	0.00207991
	5	2.97235e-12	2.97509e-08	4.76128e-07	7.62177e-06	0.00012208	0.001959125
4	0	8.55284e-12	8.54805e-08	1.36811e-06	2.19055e-05	-0.00653721	-0.01939731
	1	8.0744e-12	8.08272e-08	1.29405e-06	2.07377e-05	0.000851247	0.009479692
	2	7.64425e-12	7.65411e-08	1.22559e-06	1.96405e-05	0.000315321	0.005075537
	3	6.89296e-12	6.89818e-08	1.10411e-06	1.76848e-05	0.000283957	0.00459411
	4	6.64191e-12	6.65243e-08	1.06545e-06	1.70819e-05	0.000274468	0.004419
	5	6.04437e-12	6.04973e-08	9.68339e-07	1.55111e-05	0.000249098	0.004031459
5	0	1.45982e-11	1.45962e-07	2.33472e-06	3.7378e-05	-0.00651169	-0.01613871
	1	1.3915e-11	1.39271e-07	2.2307e-06	3.57552e-05	0.001229907	0.01454103
	2	1.32416e-11	1.32511e-07	2.12089e-06	3.39414e-05	0.000544295	0.00877038
	3	1.20846e-11	1.20922e-07	1.93648e-06	3.104e-05	0.000499478	0.008134468
	4	1.17181e-11	1.17292e-07	1.8776e-06	3.00495e-05	0.000482093	0.007770478
	5	1.07652e-11	1.07727e-07	1.7253e-06	2.76585e-05	0.000445217	0.007256343

A.4 Exact KS Potential and LDA and GGA Approximations

In the electron-He+ scattering problem, the exact KS potential has a coulomb tail but the LDA and GGA approximations are both short ranged potential, so the phase shifts can not be compared. We must compare the differential cross sections.

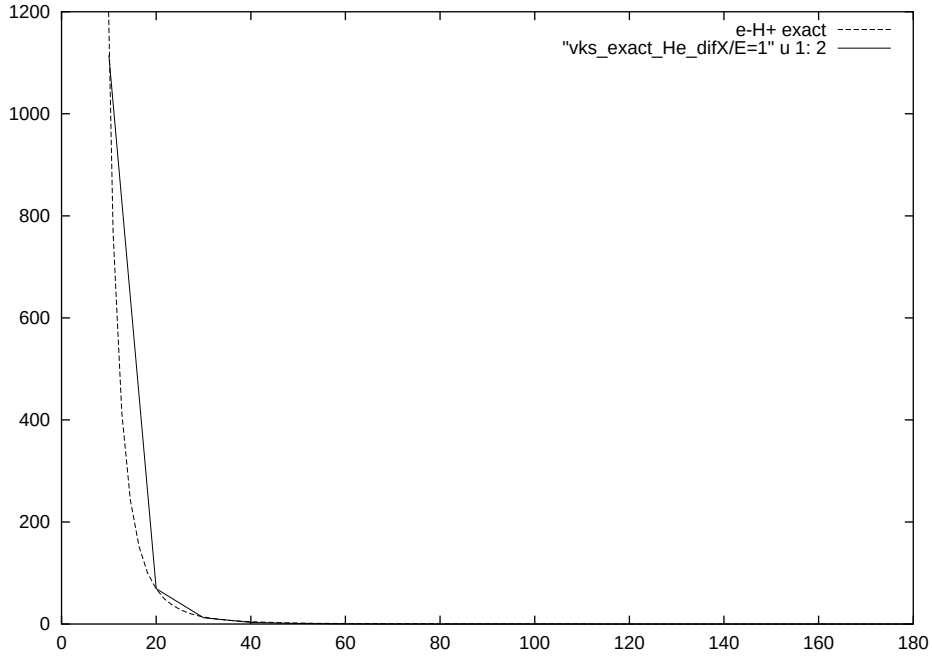

Figure A.1: Differential cross section of e-He+ with E=1. Calculations are done with the exact KS potential.

The results are shown in Figs. A.1 and A.2. Both results are calculated with $E = 1$, $L_{max} = 10$ and $\Delta x = 0.001$. The results change only a little when L_{max} and $\Delta x = 0.001$ change. It seems that the exact KS potential and LDA or GGA potential gives very differnt differential cross sections.

From Eq. (6.23), we can see that $f(\theta)$ is the summation of coulomb part and phase shift part, when $\theta \to 0$, the coulomb part goes to ∞ as $1/\theta^2$, but the phase shift part only goes to a finite value due to the fact $\delta l \to 0$ as $l \to \infty$. So $f(\theta)$ is dominated by the coulomb part, then the differential cross section is very close to

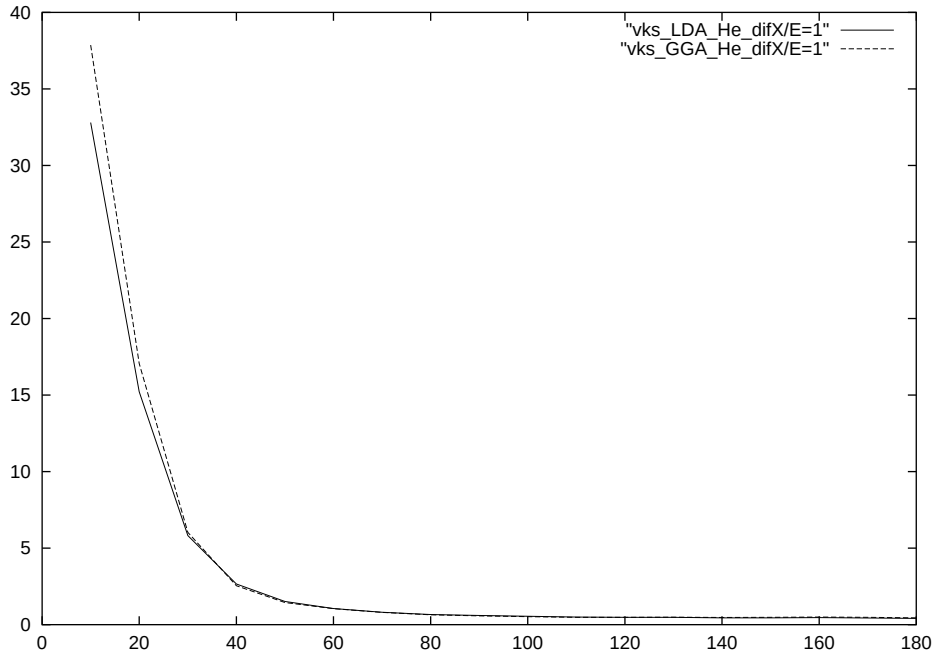

Figure A.2: Differential cross section of e-He+ with $E = 1$. Calculations are done with LDA and GGA potentials.

the coulomb scattering cross section, $\sigma(\Omega) \sim 1/\sin^4(\theta/2)$ as $\theta \to 0$. In Fig. A.1, the coulomb scattering cross section is also plotted as the dashed line, so we can see that when θ is small, the results from exact KS potential is close the the pure coulomb scattering result.

On the other hand, the differential cross section of short ranged potential is determined by Eq. (6.15). When $\theta \to 0$, the cross section should go to a finite value, not ∞.

So the short ranged potential and coulomb tailed potential can not give similar differential cross section.

It does not converge when we integrate the coulomb differential cross section, so we can not compare the total cross sections.

A.5 Test of Truncated Coulomb Potential

The truncated Coulomb potential are defined as

$$V(r) = \begin{cases} -\frac{1}{r} + \frac{1}{r_0}, & (0 < r \leq r_0), \\ 0, & (r > r_0). \end{cases} \tag{A.19}$$

It is a short ranged potential. The differential cross sections are calculated for several r_0. When r_0 become larger, the phase shift δ_l goes to 0 slower, so larger l is needed in the calculation to get accurate result. And also in Eq. (6.15), more terms will contribute to the summation. Although the differential cross section is still a finite number at $\theta = 0$, it becomes larger when r_0 increases, that makes it looks more like the exact Coulomb scattering, which goes to ∞ when $\theta \to 0$.

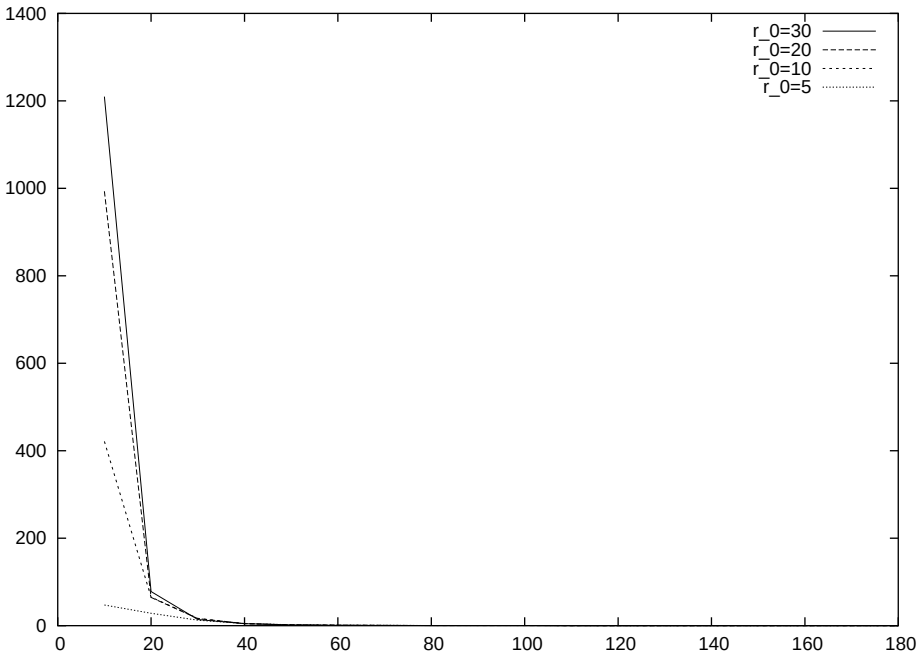

Figure A.3: Differential cross sections of e-H+ with E=1. Calculations are done using truncated Coulomb potential.

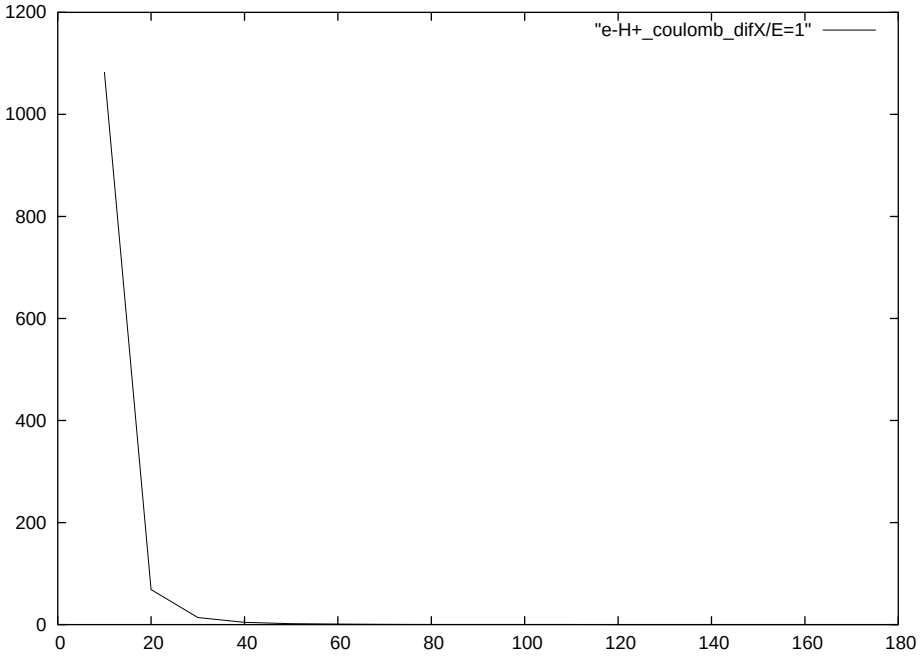

Figure A.4: Differential cross section of pure Coulomb scattering with $E = 1$.

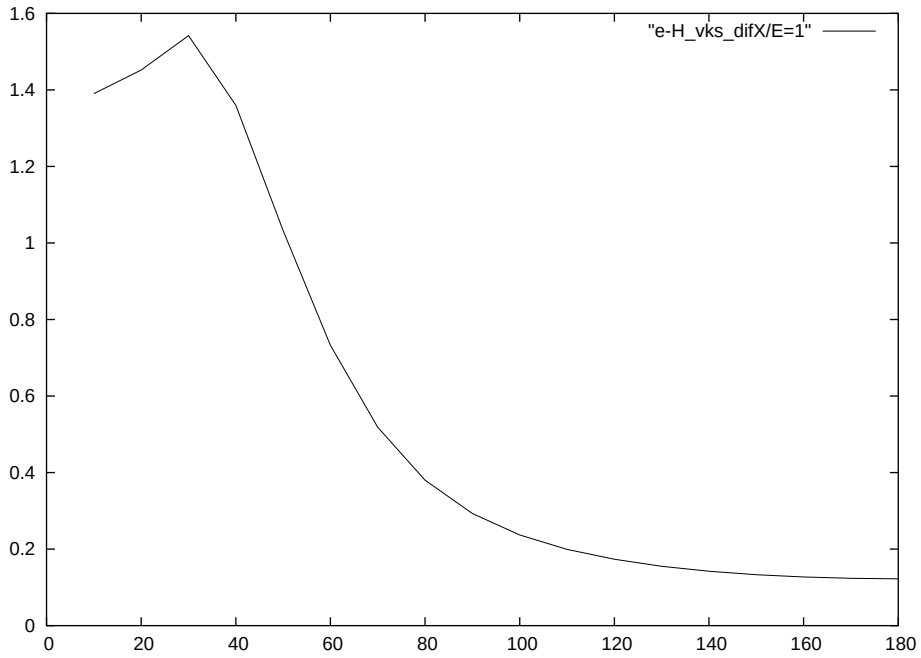

Figure A.5: Differential cross section of e-H atom scattering with E=1. Calculations are done with the KS potential of H-.

References

[1] W. Koch and M.C. Holthausen, *A Chemist's Guide to Density Functional Theory*, (New York, Wiley-VCH, 2000).

[2] P.Hohenberg & W. Kohn, Phys. Rev. B **136**, 864 (1964).

[3] W. Kohn and L.J. Sham, Phys. Rev. **140**, A 1133 (1965).

[4] W. Kohn, Rev. Mod. Phys. **71**, 1253 (1999).

[5] J. Pople in *Nobel Lectures, Chemistry 1996-2000*, ed. I. Grenthe, World Scientific Publishing Co., Singapore (2003).

[6] C.J.H. Jacobsen, S. Dahl, B.S. Clausen, S. Bahn, A. Logadottir, and J.K. Nørskov,

[7] C.J. Cramer, *Essentials of computational chemistry: theories and models*, ed. John Wiley & Sons, Inc., Chichester, England (2002).

[8] D.R. Hartree, Proc. Cambridge Phil. Soc. **24**, 89, 111, 426 (1928).

[9] C.C.J. Roothaan, Rev. Mod. Phys. **23**, 69 (1951).

[10] A. Szabo and N.S. Ostlund, *Modern Quantum Chemistry*, (New York, Macmillan, 1982).

[11] M. Head-Gordon, J.A. Pople, and M. Frisch, J. Chem. Phys. Lett. **153**, 503 (1988).

[12] R. Krishnan, M.J. Frisch, and J.A. Pople, J. Chem. Phys. **72**, 4244 (1980).

[13] J.A. Pople, M. Head-Gordon, and K. Raghavachari, J. Chem. Phys. **87**, 5968 (1987).

[14] G.D. Purvis and R.J. Bartlett, J. Chem. Phys. **76**, 1910 (1982).

[15] Gaussian 98 (Revision A.5), MJ Frisch, GW Trucks, HB Schlegel, GE Scuseria, MA Robb, JR Cheeseman, VG Zakrzewski, JA Montgomery, RE Stratmann, JC Burant, S Dapprich, JM Millam, AD Daniels, KN Kudin, MC Strain, O Farkas, J Tomasi, V Barone, M Cossi, R Cammi, B Mennucci, C Pomelli, C Adamo, S Clifford, J Ochterski, GA Petersson, PY Ayala, Q Cui, K Morokuma, DK Mailick, AD Rabuck, K Raghavachari, JB Foresman, J

Cioslowski, JV Ortiz, BB Stefanov, G Liu, A Liashenko, P Piskorz, I Komaromi, R Gomperts, RL Martin, DJ Fox, T Keith, MA Al-Laham, CY Peng, A Nanayakkara, C Gonzalez, M Challacombe, PMW Gill, BG Johnson, W Chen, MW Wong, JL Andres, M Head-Gordon, ES Replogle, JA Pople. Pittsburgh, PA: Gaussian Inc., 1998.

[16] Gaussian 03, Revision B.02, M. J. Frisch, G. W. Trucks, H. B. Schlegel, G. E. Scuseria, M. A. Robb, J. R. Cheeseman, J. A. Montgomery, Jr., T. Vreven, K. N. Kudin, J. C. Burant, J. M. Millam, S. S. Iyengar, J. Tomasi, V. Barone, B. Mennucci, M. Cossi, G. Scalmani, N. Rega, G. A. Petersson, H. Nakatsuji, M. Hada, M. Ehara, K. Toyota, R. Fukuda, J. Hasegawa, M. Ishida, T. Nakajima, Y. Honda, O. Kitao, H. Nakai, M. Klene, X. Li, J. E. Knox, H. P. Hratchian, J. B. Cross, C. Adamo, J. Jaramillo, R. Gomperts, R. E. Stratmann, O. Yazyev, A. J. Austin, R. Cammi, C. Pomelli, J. W. Ochterski, P. Y. Ayala, K. Morokuma, G. A. Voth, P. Salvador, J. J. Dannenberg, V. G. Zakrzewski, S. Dapprich, A. D. Daniels, M. C. Strain, O. Farkas, D. K. Malick, A. D. Rabuck, K. Raghavachari, J. B. Foresman, J. V. Ortiz, Q. Cui, A. G. Baboul, S. Clifford, J. Cioslowski, B. B. Stefanov, G. Liu, A. Liashenko, P. Piskorz, I. Komaromi, R. L. Martin, D. J. Fox, T. Keith, M. A. Al-Laham, C. Y. Peng, A. Nanayakkara, M. Challacombe, P. M. W. Gill, B. Johnson, W. Chen, M. W. Wong, C. Gonzalez, and J. A. Pople, Gaussian, Inc., Pittsburgh PA, 2003.

[17] J. P. Perdew and Y. Wang, Phys. Rev. B **45**, 13244 (1992).

[18] J.P. Perdew, K. Burke, and M. Ernzerhof, Phys. Rev. Lett. **77**, 3865 (1996); **78**, 1396 (1997) (E).

[19] E. Runge and E.K.U. Gross, Phys. Rev. Lett. **52**, 997 (1984).

[20] M.E. Casida, in *Recent developments and applications in density functional theory*, ed. J.M. Seminario (Elsevier, Amsterdam, 1996).

[21] K. Burke, M. Petersilka, and E.K.U. Gross in *Recent advances in density functional methods*, eds. V. Barone, A. Bencini, and P. Fantucci, World Scientific (2002), p. 67.

[22] A.D. Becke, J. Chem. Phys. **98**, 1372 (1993).

[23] A.D. Becke, J. Chem. Phys. **98**, 5648 (1993).

[24] M. Levy and J.P. Perdew, Phys. Rev. A **32**, 2010 (1985).

[25] I.N. Levine, *Quantum Chemistry*, (Boston, Allyn and Bacon, 1974).

[26] J.P. Perdew and S. Kurth, in *Density functionals: Theory and applications*, ed. D. Joubert (Springer, Berlin, 1998).

[27] R.J. Magyar, T.K. Whittingham, and K. Burke, Phys Rev A **66**, 022105 (2002).

[28] U. von Barth and L. Hedin, J. Phys. C **5**, 1629 (1972).

[29] Rajagopal, A.K, Calloway, Phys. Rev. B **7**, 1912-1919 (1973)

[30] D.C. Langreth and J.P. Perdew, Solid State Commun. **17**, 1425 (1975).

[31] O. Gunnarsson and B.I. Lundqvist, Phys. Rev. B **13**, 4274 (1976).

[32] K. Burke, M. Ernzerhof, and J.P. Perdew, Chem. Phys. Lett. **265**, 115 (1997).

[33] J.P. Perdew, M. Ernzerhof, and K. Burke, J. Chem. Phys. **105**, 9982 (1996).

[34] Y.A. Wang, Phys. Rev. A, **56**, 1646 (1997).

[35] K. Burke in *Electronic Density Functional Theory: Recent Progress and New Directions*, eds. J.F. Dobson, G. Vignale, and M.P. Das (Plenum, NY, 1997), page 19.

[36] A. D. Becke, Phys. Rev. A 38, 3098-3100 (1988).

[37] C. Lee, W. Yang, and R.G. Parr, Phys. Rev. B **37**, 785 (1988).

[38] J. P. Perdew and A. Zunger, Phys. Rev. B **23**, 5048 (1981).

[39] C.J. Umrigar and X. Gonze, Pys. Rev. A, **50**, 3827 (1994).

[40] D. Frydel, W. Terilla, and K. Burke, J. Chem. Phys. **112**, 5292 (2000).

[41] E. Davidson, S. Hagstrom, S. Chakravorty, V. Umar, and F. Fischer, Pys. Rev. A, **44**, 7071 (1991).

[42] R.C. Morrison, and Q. Zhao, Phys. Rev. A **51**, 1980 (1995).

[43] K. Burke, J.P. Perdew, and M. Ernzerhof, in *Electronic Density Functional Theory: Recent Progress and New Directions*, eds. J.F. Dobson, G. Vignale, and M.P. Das (Plenum, NY, 1997), page 57.

[44] A. Görling and M. Levy, Phys. Rev. A **50**, 196 (1994).

[45] P. Süle, Chem. Phys. Lett. **259**, 69 (1996).

[46] K. Burke, F.G. Cruz, and K.C. Lam, J. Chem. Phys. 109, 8161 (1998).

[47] A. Görling and M. Levy, Phys. Rev. A **45**, 1509 (1992).

[48] K. Burke, J. P. Perdew, and M. Levy, in *Modern Density Functional Theory: A Tool for Chemistry*, edited by J. M. Seminario and P. Politzer (Elsevier, Amsterdam, 1995).

[49] R.O. Jones and O. Gunnarsson, Rev. Mod. Phys. **61**, 689 (1989).

[50] N. T. Maitra, K. Burke, H. Appel, E.K.U. Gross, and R. van Leeuwen, in *Reviews in Modern Quantum Chemistry: A celebration of the contributions of R. G. Parr*, ed. K. D. Sen, (World-Scientific, 2001).

[51] M. Petersilka, U.J. Gossmann, and E.K.U. Gross, Phys. Rev. Lett. **76**, 1212 (1996).

[52] M. Petersilka, E.K.U. Gross, and K. Burke, Int. J. Quantum Chem. **80**, 534 (2000).

[53] R.J. Cave, F. Zhang, N.T. Maitra, and K. Burke, Chem. Phys. Lett. **389**, 39 (2004)

[54] R.G. Parr and W. Yang (Oxford, New York, 1989).

[55] Y.A. Wang, Phys. Rev. A **56**, 1646 (1997).

[56] E.R. Davidson, S.A. Hagstrom, S.J. Chakravorty, V. Meiser Umar, and C. Froese Fischer, Phys. Rev. A **44**, 7071 (1991).

[57] S.J. Chakravorty, S.R. Gwaltney, E.R. Davidson, F.A. Parpia, and C. Froese Fischer, Phys. Rev. A **47**, 3649 (1993).

[58] E. Engel and R.M. Dreizler, J. Comput. Chem. **20**, 31 (1999).

[59] C.J. Huang and C.J. Umrigar, Phys. Rev. A **56**, 290 (1997).

[60] M. Levy, Phys. Rev. A **43**, 4637 (1991).

[61] J. Harris and R.O. Jones, J. Phys. F **4**, 1170 (1974).

[62] D.C. Langreth and J.P. Perdew, Phys. Rev. B **15**, 2884 (1977).

[63] A. Görling and M. Levy, Phys. Rev. B **47**, 105 (1993).

[64] E.R. Davidson, Int. J. Quant. Chem. **69**, 241 (1998).

[65] A. Görling and M. Ernzerhof, Phys. Rev. A **51**, 4501 (1995x).

[66] E.P. Ivanova and U.I. Safronova, J. Phys. B: Atom. Molec. Phys. **8**, 1591 (1975).

[67] S. Ivanov and M. Levy, J. Phys. Chem. A **102**, 3151 (1998).

[68] C. Filippi, X. Gonze, and C.J. Umrigar, in *Recent Developments and Applications of Density Functional Theory*, ed. J.M. Seminario (Elsevier, Amsterdam, 1996).

[69] E. Clementi and C. Roetti, At. Data Nucl. Data Tables **14**, 177 (1974).

[70] O. Jitrik and C.F. Bunge, Phys. Rev. A **43**, 5804 (1991).

[71] Q. Zhao and R.G. Parr, Phys. Rev. A **46**, 2337 (1992).

[72] Q. Zhao and R.G. Parr, J. Chem. Phys. **98**, 543 (1992).

[73] Q. Zhao, R.C. Morrison, and R.G. Parr, Phys. Rev. A **50**, 2138 (1994).

[74] V.N. Staroverov, G.E. Scuseria, J.P. Perdew, J. Tao, and E.R. Davidson, submitted to Phys. Rev. A (2004).

[75] Y. Wang and J.P.Perdew, Phys. Rev. B **43**, 8911 (1991).

[76] S. Ivanov, K. Burke, and M. Levy, J. Chem. Phys. **110**, 10262 (1999).

[77] A.A. Jarzecki and E.R. Davidson, Mol. Phys. **98**, 1089 (2000).

[78] A. Facco Bonetti, E. Engel, R.N. Schmid, and R.M. Dreizler, Phys. Rev. Lett. **86**, 2241 (2001).

[79] R.J. Cave, and E.R. Davidson, J. Phys. Chem. **91**, 4481 (1987).

[80] R.J. Cave, and E.R. Davidson, J. Phys. Chem. **92**, 614 (1988).

[81] B.S. Hudson, and B.E. Kohler, Ann. Rev. Phys. Chem. **25**, 437 (1974).

[82] B.S. Hudson, B.E. Kohler, and K. Shulten, *E.C.Lim (Ed.), Excited States*, Vol. 6, Academic Press, New York, p.1 (1982).

[83] C.P. Hsu, S. Hirata, and M. Head-Gordon, J. Phys. Chem. A **105**, 451 (2001).

[84] W.J. Buma, B.E. Fohler, and K. Song, J. Chem. Phys. **94**, 6367 (1991).

[85] J. Lappe, and R.J. Cave, J. Phys. Chem. A **104**, 2294 (2000).

[86] L. Serrano-Andres, M. Merchan, R. Lindh, and B. O. Roos, J. Chem. Phys. **98**, 3151 (1993).

[87] C.P. Hsu, S. Hirata, and M. Head-Gordon, J. Phys. Chem. A **105**, 451 (2001).

[88] N.T. Maitra, F. Zhang, R.J. Cave and K. Burke, J. Chem. Phys. **120**, 5932 (2004).

[89] W. Haugen, and M. Traetteberg, Acta Chem. Scand. **20**, 1726 (1966).

[90] S. Hirata, and M. Head-Gordon, Chem. Phys. Lett. **314**, 291 (1999).

[91] A. Görling, Phys. Rev. A **54**, 3912 (1996).

[92] C. Daul, Int. J. Quantum Chem. **52**, 867 (1994).

[93] M. Levy and A. Nagy, Phys. Rev. Lett. **83**, 4361 (1999).

[94] C. Filippi, C.J. Umrigar, and X. Gonze, J. Chem. Phys., **107**, 9994 (1997).

[95] J.P. Perdew, A. Savin, and K. Burke, Phys. Rev. A **51**, 4531 (1995).

[96] W. Kohn, Rev. Mod. Phys. **71**, 1253 (1999).

[97] J.P. Perdew, E.R. McMullen, & A. Zunger, Phys. Rev. A **23**, 2785 (1981).

[98] A.A. Jarzecki & E.R. Davidson, Phys. Rev. A **58**, 1902 (1998).

[99] C. Schwartz, Phys. Rev. bf 124, 553 (1961).

[100] A.K. Bhatia, Phys. Rev. A **66**, 064702 (2002).

[101] K. Burke, M. Petersilka, and E.K.U. Gross, in *Recent advances in density functional methods, vol. III*, ed. P. Fantucci and A. Bencini (World Scientific Press, 2000).

[102] http://www.gnu.org/software/gsl/

[103] E.K.U.Gross, J.F.Dobson, and M.Petersilka, Topics in Current Chemisty, **181**, 81 (1996).

[104] N.T. Maitra, A. Wasserman, and K.Burke, in Electron Correlations and Materials Properties 2, ed. A. Gonis, N. Kioussis, M. Ciftan, (Kluwer/Plenum, 2003).

[105] Q. Zhao, M. Levy, and R. Parr, Phys. Rev. A, **47**, 918 (1993).

[106] Z. Qian and V. Sahni, Phys. Rev. A **57**, 2527 (1998).

[107] C. Adamo and V. Barone, J. Chem. Phys. **110**, 6158 (1999).

[108] M.Seidl, J. Perdew, and S. Kurth, Phys. Rev. A **62**, 012502 (2000).

[109] K. Burke, J.P. Perdew, and M. Levy, Phys. Rev. A **53**, R2915 (1996).

[110] R.J. Magyar, W. Terilla, and K. Burke, J. Chem. Phys. **119**, 696 (2003).

[111] S. Kais, D.R. Herschbach, N.C. Handy, C.W. Murray, and G.J. Laming, J. Chem. Phys. **99**, 417 (1993).

[112] A. Görling and M. Levy, Phys. Rev. B **47**, 13105 (1993).

[113] A. Görling and M. Levy, Int. J. Quant. Chem. **29**, 93 (1995).

[114] J. Perdew, S. Kurth, and M. Seidl, International Journal of Modern Physics B, Vol. **15**, 1672 (2001).

[115] K. Burke, J. Perdew, and M. Ernzerhof, J. Chem. Phys. **109**, 3760 (1998).

[116] A. Savin, C. J. Umrigar, X. Gonze, Chem. Phys. Lett. **288**, 391 (1998).

[117] H. Appel, E.K.U. Gross, and K. Burke, Phys. Rev. Lett. **90**, 043005 (2003).

[118] C. J. Umrigar and X. Gonze, in *H*igh Performance Computing and its Application to the Physical Sciences, ed. D. A. Browne *e*t al., Proceedings of the Mardi Gras '93 Conference (World Scientific, Singapore, 1993).

[119] Q. Zhao, R. C. Morrison, and R. G. Parr, Phys. Rev. A **50**, 2138 (1994).

[120] A. Becke, J. Chem. Phys. **104**, 1040 (1996).

[121] A. Savin, F. Colonna, and J.-M. Teuler, in *Electronic Density Functional Theory: Recent Progress and New Directions*, eds. J.F. Dobson, G. Vignale, and M.P. Das (Plenum, NY, 1997).

[122] E.K.U. Gross and S. Kurth in *Relativistic and Electron Correlation Effects in Molecules and Solids* ed. G.L. Malli (Nato ASI Series, Plenum, 1993).

[123] *Quantum mechanics*, A. Messiah, Chap X, XI (John Wiley & sons, 1961)

[124] *Computational physics*, J. M. Thijssen, Chap. 2 (Cambridge University Press, 1999).

[125] A. Gonis, *Green Functions for Ordered and Disordered Systems*, Studies in M athematical Physics, Vol. 4, eds. E.van Groesen and E.M. de Jager, (Elsevier Sci ence Publishers B.V., North-Holland, 1992).

[126] *Theoretical Atomic Physics*, H. Friedrich, 2nd ed. (Springer-Verlag, 1998).

Curriculum Vita

Fan Zhang

EDUCATION

2005 Ph.D. in Physics, Rutgers University, New Brunswick, NJ

1999 M.S. in Physics, Peking University, P.R.China (July 1999)

1997 B.S. in Physics, Peking University, P.R.China (July 1997)

POSITIONS HELD WHILE A GRADUATE STUDENT

2002-2005 Graduate Assistant, Rutgers University Department of Physics and Astronomy
2001-2002 Teaching Assistant, Rutgers University Department of Physics and Astronomy
1999-2001 Fellow, Rutgers University

PUBLICATIONS

Adiabatic connection for near degenerate excited states,
F. Zhang and K. Burke, Phys. Rev. A **69**, 052510 (2004).

A Dressed TDDFT Treatmentof the 2^1A_g *States of Butadiene and Hexatriene*,
R.J. Cave, F. Zhang, N.T. Maitra, and K. Burke, Chem. Phys. Lett. **389**, 39 (2004).

Double excitations in time-dependent density functional theory linear response,
N.T. Maitra, F. Zhang, R.J. Cave, and K. Burke, J. Chem. Phys. **129**, 5932 (2004).